CU-TP-1104

Small-x physics beyond the Kovchegov equation*

A. H. Mueller [a] and A. I. Shoshi [b]

Physics Department, Columbia University, New York, NY 10027, USA

Abstract

We note the differences between the Kovchegov equation and the Balitsky-JIMWLK equations as methods of evaluating high energy hard scattering near the unitarity limit. We attempt to simulate some of the correlations absent in the Kovchegov equation by introducing two boundaries rather than the single boundary which effectively approximates the unitarity limit guaranteed in the Kovchegov equation. We solve the problem of BFKL evolution in the presence of two boundaries and note that the resulting T-matrix now is the same in different frames, which was not the case in the single boundary case. The scaling behavior of the solution to the Kovchegov equation is apparently now lost.

Keywords: Saturation momentum, scaling region, Kovchegov equation, Balitsky equation, JIMWLK equation, BFKL equation, saturation line

PACS numbers: 11.80.Fv, 12.38.-t, 12.40.-y, 13.60.-r,

*This work is supported in part by the US Department of Energy.

[a]arb@phys.columbia.edu (A.H.Mueller)

[b]shoshi@phys.columbia.edu

1 Introduction

Scattering at the unitarity limit and parton saturation [1] are dual descriptions of the same phenomenon [2] which lies at the heart of some of the most interesting parts of small-x hard scattering. The QCD dynamics giving the growth of the cross section with increasing energy, or equivalently, giving the growth of the parton density with decreasing x is BFKL [3, 4] evolution. Ordinary QCD, or DGLAP [5–7], evolution also leads to increasing parton number densities, however, in order to get large gluon occupation numbers characteristic of gluon saturation (Color Glass Condensate [8]) it is necessary that parton densities, or cross sections, grow at a fixed hard scale and this requires BFKL evolution. Understanding QCD wavefunctions having high gluon occupation number and high energy hard scattering near the unitarity limit are two seemingly different aspects of the same phenomenon. The partonic language appears to be the more interesting description because it suggests one should be able to produce quite dense QCD matter. Indeed, in a central collision of high energy heavy ions the system produced just after the collision is believed to be a system of nonequilibrium gluons at high density and high occupation numbers. This system then evolves into an equilibrated quark-gluon plasma of lower density and lower occupation numbers [9].

Of course genuine BFKL evolution is only accurate when gluon occupation numbers are not too large, or equivalently, when S-matrix elements are not too close to the unitarity limit. The Balitsky equation [10] is a generalization of the BFKL equation which should be the leading term in a systematic treatment of the dynamics of high energy hard scattering at or near the unitarity limit. An equivalent formalism was developed by Jalilian-Marian, Iancu, McLerran, Leonidov and Kovner (JIMWLK) [8, 11–13] in terms of small-x evolution of QCD wavefunctions in a light-cone gauge. The Balitsky and JIMWLK equations are coupled equations involving higher and higher correlations much as in the Schwinger-Dyson equations in ordinary perturbation theory, and as such are very difficult to deal with analytically. However, an interesting numerical calculation has recently appeared [14] and one can expect a better understanding of Balitsky and JIMWLK evolution to emerge from such calculations.

Kovchegov [15] has suggested a somewhat simpler equation than the Balitsky or JIMWLK equations to deal with scattering at or near the unitarity limit. Although Kovchegov originally derived his equation in the context of a high energy scattering on a large nucleus, this equation can also be viewed as a mean field version of the Balitsky equation in which higher correlations are neglected. For example the S-matrix for the scattering of a state of two QCD dipoles on a highly evolved target, and at a definite impact parameter, is replaced by the product of the S-matrices

of the individual dipoles. While the Kovchegov equation is not so complete it does have the advantage of being a precise nonlinear equation for a function. Many interesting limits of the Kovchegov equation have been understood by analytical methods. While incomplete, as is any mean field like approximation, the Kovchegov equation is likely the best equation one can write down in terms of functions which has built in correct unitarity limits for high energy scattering. In Sec. 3 we give a derivation of the Kovchegov equation, since its understanding plays a central role in this paper.

In kinematical regions where the scattering of a QCD dipole on a target is far from its unitarity limit the Kovchegov equation reduces to the BFKL equation. At a given impact parameter the dipole target T-matrix ($T = 1 - S$) grows with energy until it approaches 1 at which point the nonlinear part of the Kovchegov equation limits the growth of T not to be larger than 1. If $2/Q$ is the transverse size of the scattering dipole then the saturation momentum is defined to be the value of Q at which T is some preassigned number, say $1/2$. This saturation momentum is a function of rapidity Y, $Q_s(Y)$, and gives the scale separating weak and strong scattering. The transition between weak and strong scattering is expected to be rapid as one varies the scale Q. In the weak scattering region the BFKL equation can be viewed, roughly, as a product of two factors: The first gives an exponential dependence in $\rho = \ln(Q^2/\Lambda^2)$ while the second factor represents a diffusion in ρ with αY playing the role of time. In Refs. [16] and [17] it was suggested that one could get an approximate analytic solution to the Kovchegov equation simply by taking the diffusive part of the BFKL equation and imposing an absorptive boundary near $\rho_s = \ln(Q_s^2/\Lambda^2)$. This procedure was then used to evaluate in detail the Y-dependence of Q_s and the form of $T(\rho, Y)$ when $\rho > \rho_s$. These results confirmed the broad picture arrived at by less complete techniques earlier [1, 18–20]. Recently Munier and Peschanski [21] have developed a more general and more powerful procedure for studying the properties of the Kovchegov equation near the saturation boundary, confirming the corrections of the absorptive boundary approach of Refs. [16, 17] along the way.

However, the issue still remains to what extend the Kovchegov equation actually represents the Balitsky and JIMWLK equations at or near the saturation region. One exact result of the Kovchegov equation which has been known for some time is the Levin-Tuchin formula [22] for the S-matrix deep in the saturation region which states

$$S(\rho, b, Y) \sim e^{-c(\rho - \rho_s)^2} \tag{1.1}$$

where the constant $c = -C_F(1 - \lambda_0)/(N_c 2\chi(\lambda_0))$ has a value which follows from the Kovchegov equation. Recently, the authors of Ref. [23] have claimed that S deep in the saturation regime has the form given by (1.1) but with a constant at least

a factor of 2 smaller than the c which follows from the Kovchegov equation. The cause for this discrepancy is the lack of fluctuations in the Kovchegov equation. Even earlier, Salam [24] has argued on the basis of numerical simulations that fluctuations are generally large in BFKL evolution and so there is no reason to expect that they will be small near the saturation boundary.

It is not hard to see that fluctuations are potentially important in evolution not too far from the saturation boundary. As an example consider the high-energy scattering of a dipole of size ρ_f at rapidity Y on a dipole of size ρ_i at zero rapidity. (The relation between ρ and the transverse size $x_\perp$ of a dipole is $\rho = \ln(4/\Lambda^2 x_\perp^2)$.) We may view the problem in terms of BFKL evolution with $\rho > \rho_s(y)$ with the boundary near $\rho_s(y)$ constituting an absorptive boundary for diffusion inherent in BFKL evolution. Further the evolution can be viewed as an evolution from $(\rho_i,\, 0)$ to an intermediate point $(\rho,\, y)$ and then from $(\rho,\, y)$ to $(\rho_f,\, Y)$. We expect the final answer [19] to be close to $T(\rho_i \to \rho_f) \sim e^{-(1-\lambda_0)(\rho_f - \rho_s(Y))}$. In terms of the evolution through the intermediate point $(\rho,\, y)$ we can write

$$T(\rho_i \to \rho_f) \sim \int_{\rho_1(y)}^{\infty} d\rho\, T(\rho_i \to \rho)\, T(\rho \to \rho_f) \tag{1.2}$$

at least as far as the exponential factors are concerned. The T's in (1.2) are all defined by BFKL evolution with an absorbtive boundary in ρ at $\rho_1(y)$, near $\rho_s(y)$. Fig. 1 shows in the ρ - Y plane the boundaries and the shaded saturation region limiting the BFKL evolution. Clearly $T(\rho_i \to \rho) \sim e^{-(1-\lambda_0)(\rho - \rho_s(y))}$ so one would expect that values of ρ in (1.2) such that $\rho - \rho_s(y) > \rho_f - \rho_s(Y)$ would contribute little to the integral on the right hand side of (1.2). This should be the case since according to unitarity $T(\rho \to \rho_f)$ should not be larger than 1, however, such is not the case. The dominant contribution to the right-hand side of (1.2) comes from regions with $\rho - \rho_s(y) > \rho_f - \rho_s(Y)$ where manifestly $T(\rho \to \rho_f) \gg 1$. This occurs because the boundary for $T(\rho \to \rho_f)$ is matched to the boundary for $T(\rho_i \to \rho)$, as shown in Fig. 1, in order to get the same answer from both sides of eq. (1.2). There is unitarity violating evolution also in the region with $\rho - \rho_s(y) < \rho_f - \rho_s(Y)$ when the evolution goes from one intermediate point to another before it ends at the final point. For (1.2) to be a correct formula and in order to guarantee unitarity respecting amplitudes for each path of evolution the saturation boundary for $T(\rho \to \rho_f)$ should follow the value of ρ and thus it should not be the same as for $T(\rho_i \to \rho)$. In this case, the BFKL evolution with a saturation boundary does not fulfill (1.2).

In this work we introduce a second absorptive barrier at $\rho = \rho_2(y)$, as shown in Fig. 2, such that, crudely, $T(\rho \to \rho_f) \leq 1$ when $\rho < \rho_2$. This second boundary eliminates all unitarity violating evolution between the initial point $(\rho_i,\, 0)$ and the final point $(\rho_f,\, Y)$ when the evolution is viewed as proceeding in two steps; from the initial point $(\rho_i,\, 0)$ to an intermediate point $(\rho,\, y)$ and then from the intermediate

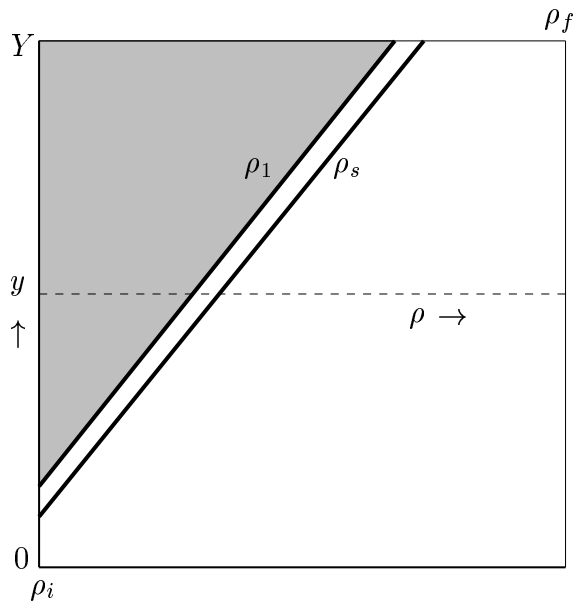

Figure 1: BFKL evolution in the presence of one saturation boundary.

point (ρ, y) to the final point (ρ_f, Y). However, when the evolution is viewed as proceeding through two or more intermediate steps, $(\rho_i, 0) \rightarrow (\rho, y) \rightarrow (\rho', y' > y) ... \rightarrow (\rho_f, Y)$, then the second boundary $\rho_2(y)$ does not eliminate all unitarity violating evolution between one intermediate point and another, i.e., $T(\rho \rightarrow \rho')$ may become larger than 1. The remaining unitarity violating evolution cannot be eliminated without going back to the Balitsky or JIMWLK equations.

The boundary ρ_1 is the boundary corresponding to saturation in the wavefunction of the evolved dipole ρ_i. This boundary is naturally viewed as an approximate way of imposing the unitarity limit given by the Kovchegov equation when the scattering is viewed as the scattering of an elementary dipole ρ_f on a highly evolved dipole ρ_i. However, we may also view the process as the scattering of an elementary dipole ρ_i on the evolved dipole ρ_f. When $\rho_f > \rho_i$ one calls this evolution a backward evolution, and it has previously been used [25] in studying shadowing effects in scattering on nuclei. The Kovchegov equation in this backward evolution is imposed approximately in terms of the boundary ρ_2. There is in fact a complete symmetry here; the boundary ρ_1 is to ρ_i in forward evolution as the boundary ρ_2 is to ρ_f in backward evolution (see Fig. 2).

The introduction of the second boundary ρ_2 and the resulting symmetry which it brings with it has another benefit. The scattering amplitude is now boost invariant which was not the case for the single boundary case. Thus the calculation in the

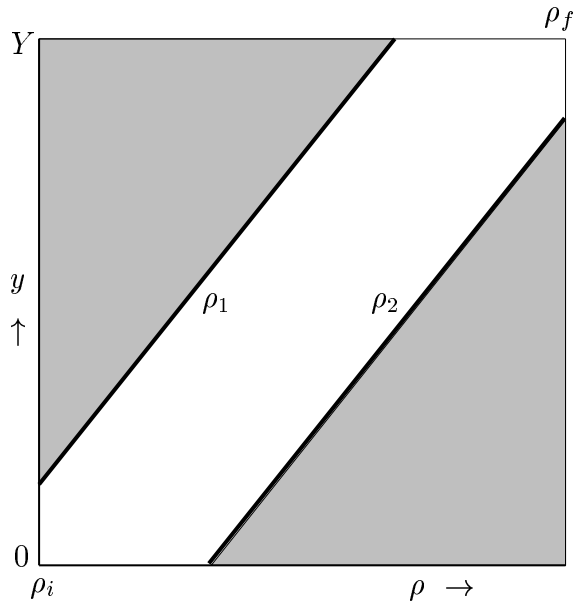

Figure 2: BFKL evolution in the presence of two saturation boundaries.

center of mass, say, now gives the same answer as arises when all the evolution is put into one or the other of the two dipoles.

The paper is organized as follows: Sec. 2 gives some results from dipole-dipole scattering in the BFKL approximations. In Sec. 3 the Kovchegov equation is derived emphasizing the "mean field" aspects necessary for the derivation. The approximate solution is given in the absorptive boundary approximation. The frame-dependence of scattering is demonstrated. In Sec. 4 the second boundary, ρ_2, is introduced and the BFKL equation is solved in the presence of the two boundaries in the diffusion approximation. The positions of the boundaries and the energy dependence of the saturation momentum are determined. In Sec. 5 the discussion of Sec. 4 is repeated for running coupling evolution.

In Sec. 4 and Sec. 5 we have solved the BFKL equations, with boundaries ρ_1 and ρ_2, in a diffusion approximation. Perhaps the main change from the single boundary case is that the scaling law which follows from the Kovchegov equation is now badly violated as explained at the end of Sec. 4.2. The effect of the two boundaries, as compared to the single boundary, is parametrically small but in practice very large. For example the anomalous dimension λ_0 becomes λ_d where

$$\lambda_d = \lambda_0 + \frac{1}{2(1-\lambda_0)} \frac{\pi^2}{(\rho_2 - \rho_1)^2} \tag{1.3}$$

and where $\rho_2 - \rho_1 \approx \ln 1/\alpha^2 + \rho_f - \rho_{is}(Y)$ (ρ_{is} is the saturation line for internal evolution), parametrically. Indeed the resulting corrections are so large that one may well doubt the diffusion approximation we have used. It's possible that our procedure has overcorrected the deficiencies of the Kovchegov equation, although our second boundary only eliminates paths of evolution which manifestly violate unitarity. It would be interesting to do a numerical solution of BFKL evolution in the presence of two boundaries to see if the diffusion approximation is accurate.

We feel that the main conclusion of this study is that correlations may be very important near the saturation boundary and in the scaling region. The best way to see if this is really true, and to see if our procedure of calculation has hit the essence of the physics, is to do accurate numerical simulations of the JIMWLK equation as already begun in Ref. [14] to see how different those results are from those of the Kovchegov equation and from our two boundary procedure of imposing unitarity.

2 Dipole-Dipole scattering; general definitions

In this section we give some general formulas and definitions concerning the dipole-dipole scattering which will be used throughout this work.

Suppose we consider the scattering of a dipole of size x on a dipole of size x' at relative rapidity Y. In a frame where one of the dipoles has rapidity y and the other has rapidity $Y - y$, the forward scattering amplitude is given by

$$T(x, x', Y) = \int \frac{d^2 r_1 d^2 r_2}{4\pi^2 r_1^2 r_2^2}\; n(x, r_1, y)\; n(x', r_2, Y - y)\; \sigma_{dd}(r_1, r_2) \tag{2.1}$$

where $\sigma_{dd}(r_1, r_2)$ is the dipole-dipole cross section at the two gluon exchange level

$$\sigma_{dd}(r_1, r_2) = 2\pi\alpha^2 r_<^2 \left(1 + \ln \frac{r_>}{r_<}\right)\ , \tag{2.2}$$

with $r_<$ being the smaller of r_1, r_2 and $r_>$ being the larger of r_1, r_2 while $n(x, r_1, y)$ is the number density of radiated dipoles of size r_1 in the wavefunction of a parent dipole of size x in the rapidity interval y. The expression for $n(x, r_1, y)$ which obeys the dipole version of the BFKL equation reads for $x > r_1$ [26]

$$n(x, r_1, y) = 2\left(\frac{x^2}{r_1^2}\right) \int \frac{d\lambda}{2\pi i}\; \exp\left[\frac{2\alpha N_c}{\pi}\chi(\lambda) y - (1 - \lambda)\ln\frac{x^2}{r_1^2}\right] \tag{2.3}$$

and for $x < r_1$

$$n(x, r_1, y) = 2 \int \frac{d\lambda}{2\pi i}\; \exp\left[\frac{2\alpha N_c}{\pi}\chi(\lambda) y - (1 - \lambda)\ln\frac{r_1^2}{x^2}\right] \tag{2.4}$$

or

$$n(x, r_1, y) = \left(\frac{x^2}{r_1^2}\right) n(r_1, x, y) \quad (\text{for } x < r_1) \ , \tag{2.5}$$

where

$$\chi(\lambda) = \psi(1) - \frac{1}{2}\psi(\lambda) - \frac{1}{2}\psi(1-\lambda) \tag{2.6}$$

with $\psi(\lambda) = \Gamma'(\lambda)/\Gamma(\lambda)$. The integration contour in eqs. (2.3) and (2.4) is parallel to the imaginary axis with $0 < \mathrm{Re}(\lambda) < 1$.

The scattering amplitude in eq. (2.1) can be evaluated in an arbitrary frame since the result does not depend on the frame. Often the evalution of the amplitude becomes especially easy in the laboratory frame where one of the dipoles carries all of the rapidity (this dipole evolves) and the other one has zero rapidity (this dipole is an elementary dipole). In this case, for $y = Y$, the integration over r_2 can be done because $n(x', r_2, 0) = r_2 \delta(r_2 - x')$ and the result is

$$T(x, x', Y) = \int \frac{d^2 r_1}{2\pi r_1^2} \ n(x, r_1, Y) \ \sigma_{dd}(r_1, x') \ . \tag{2.7}$$

Inserting (2.2) and (2.3) in (2.7), also the integration over r_1 can be easily done,

$$\int \frac{d^2 r_1}{2\pi r_1^2} \left(\frac{x^2}{r_1^2}\right)^{\lambda} \ 2\pi\alpha^2 r_<^2 \left(1 + \ln\frac{r_>}{r_<}\right) = \frac{\pi}{2}\alpha^2 x'^2 \left(\frac{x^2}{x'^2}\right)^{\lambda} \frac{1}{\lambda^2(1-\lambda)^2} \ , \tag{2.8}$$

leading to

$$T(x, x', Y) = \pi\alpha^2 x'^2 \int \frac{d\lambda}{2\pi i} \frac{1}{\lambda^2(1-\lambda)^2} \exp\left[\frac{2\alpha N_c}{\pi}\chi(\lambda) Y - (1-\lambda)\ln\frac{x^2}{x'^2}\right] \left(\frac{x^2}{x'^2}\right) \ . \tag{2.9}$$

3 The Kovchegov equation and its limitations

In this section we "derive" the Kovchegov equation [15] which is probably the best "simple" equation including nonlinear evolution in QCD. An analytic solution to the Kovchegov equation in the region close to the saturation regime has been recently achieved [21]; analytic results for the scattering amplitude in laboratory frame and for the saturation momentum as a function of rapidity are obtained. These results agree with the ones obtained before by solving the linear BFKL equation in the presence of a saturation boundary [16]. In this work, we show that the scattering amplitude in the vicinity of the saturation regime which results from the Kovchegov equation does not satisfy the completeness relation and it is frame-dependent.

3.1 The Kovchegov equation

Consider the high-energy scattering of a quark-antiquark dipole on a target which may be another dipole, a hadron or a nucleus. For convenience we view the scattering process in a frame where the dipole is left moving and the target is right moving. Further we suppose that almost all of the relative rapidity of the dipole and the target, Y, is taken by the target so that the probability for the left-moving dipole to emit gluons before scattering off the target is small. In this frame an elementary quark-antiquark dipole scatters on a highly evolved target. We denote the corresponding elastic scattering amplitude by $S(\underline{x}_0, \underline{x}_1, Y)$ where $\underline{x}_0$ and $\underline{x}_1$ are the transverse coordinates of the quark and antiquark of the dipole, respectivelly. Now we wish to know how $S(\underline{x}_0, \underline{x}_1, Y)$ changes when the rapidity Y is increased by a small amount dY. The increase dY can be viewed either as increasing the momentum of the target or as increasing the momentum of the elementary dipole. If the rapidity of the target is increased than its wavefunction evolves further. This evolution is given by the functional equation derived by Jalilian-Marian, Iancu, McLerran, Leonidov and Kovner (JIMWLK) [11–13]. On the other hand, if the rapidity of the dipole is increased while that of the target is kept fixed, the probability for the dipole to emit a gluon increases (proportional to dY) due to the change dY. In the large N_c limit this quark-antiquark-gluon state can be viewed as a system of two dipoles – one of the dipoles consists of the initial quark and the antiquark part of the gluon while the other dipole is given by the quark part of the gluon and the initial antiquark. The probability for the production of a quark-antiquark-gluon state from the initial quark-antiquark dipole is [27]

$$dP = \frac{\alpha N_c}{2\pi^2} d\underline{x}_2 dY \frac{\underline{x}_{01}^2}{\underline{x}_{02}^2 \underline{x}_{12}^2} \ , \tag{3.1}$$

where $\underline{x}_2$ is the transverse coordinate of the emitted gluon while $\underline{x}_{01}$, $\underline{x}_{02}$ and $\underline{x}_{12}$ with $\underline{x}_{ij} = \underline{x}_i - \underline{x}_j$ are the transverse sizes of the dipoles as shown in Fig. 3. The probability dP when multiplied with the S-matrix for the two dipole state to elastically scatter on the target gives the change in the S-matrix, dS, for dipole-hadron scattering

$$\frac{\partial}{\partial Y} S(\underline{x}_{01}, Y) = \frac{\alpha N_c}{2\pi^2} \int d^2\underline{x}_2 \frac{\underline{x}_{01}^2}{\underline{x}_{02}^2 \underline{x}_{12}^2} \left[S^{(2)}(\underline{x}_{02}, \underline{x}_{12}, Y) - S(\underline{x}_{01}, Y) \right] \ . \tag{3.2}$$

Here $S^{(2)}(\underline{x}_{02}, \underline{x}_{12}, Y)$ stands for the scattering of the two dipole state on the target (first graph on the left-hand side of Fig. 3) while the subtracted $S(\underline{x}_{01}, Y)$ is the virtual contribution necessary to normalize the wavefunction [27, 28]. The later gives the scattering of a single dipole on the target because the gluon is not in the wavefunction of the dipole at the time of the scattering (last two graphs in Fig. 3).

Eq. (3.2) is part of a set of equations derived by Balitsky [10] and it also results from the JIMWLK functional equations [12, 13]. It is difficult to use eq. (3.2) because

of the unknown $S^{(2)}(\underline{x}_{02}, \underline{x}_{12}, Y)$. The assumption that the scattering of the two dipole state on the target factorizes

$$S^{(2)}(\underline{x}_{02}, \underline{x}_{12}, Y) = S(\underline{x}_{02}, Y) S(\underline{x}_{12}, Y) \ , \tag{3.3}$$

which is a sort of a mean field approximation for the gluonic fields in the target, leads to the Kovchegov equation [15]

$$\frac{\partial}{\partial Y} S(\underline{x}_{01}, Y) = \frac{\alpha N_c}{2\pi^2} \int d^2\underline{x}_2 \frac{\underline{x}_{01}^2}{\underline{x}_{02}^2 \underline{x}_{12}^2} \left[S(\underline{x}_{02}, Y) S(\underline{x}_{12}, Y) - S(\underline{x}_{01}, Y) \right] \ . \tag{3.4}$$

This equation is probably the best "simple" equation taking into account unitarity corrections. In his original works [15] Kovchegov used the approximation (3.3) for the case that the target is a large nucleus. In this case, eq. (3.3) is a reasonable approximation. The factorization (3.3) is however less obvious for an arbitrary target. It is the mean field approximation (or factorization) which makes the Kovchegov equation treat fluctuations incorrectly. In the region where S is small, it has been shown in Ref. [23] that the Kovchegov equation, while giving the form of the S-matrix correctly, gives the exponential factor twice as large as the result which emerges when flutuations are taken into account. Furthermore, in the next subsections, we show that the scattering amplitude which results from the Kovchegov equation is not consistent with the completeness relation and it is frame-dependent. This is because the evolution of the amplitude in rapidity is devided into two successive steps in both cases and at the intermediate step fluctuations are not properly taken into account.

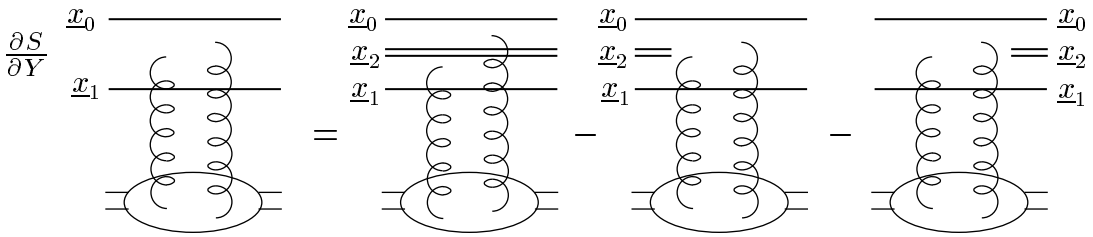

Figure 3: Graphs corresponding to terms in the Kovchegov equation.

Using $\mathcal{N}(\underline{x}_{ij}, Y) = 1 - S(\underline{x}_{ij}, Y)$, another useful version of the Kovchegov equation follows

$$\frac{\partial}{\partial Y} N(\underline{x}_{01}, Y) = \frac{\alpha N_c}{2\pi^2} \int d^2\underline{x}_2 \frac{\underline{x}_{01}^2}{\underline{x}_{02}^2 \underline{x}_{12}^2} \ \left[N(\underline{x}_{02}, Y) + N(\underline{x}_{12}, Y) \right.$$
$$\left. - N(\underline{x}_{01}, Y) - N(\underline{x}_{02}, Y) N(\underline{x}_{12}, Y) \right] \ . \tag{3.5}$$

This equation becomes easy to use when the scattering is weak since the nonlinear term $N(\underline{x}_{02}, Y)N(\underline{x}_{12}, Y)$ can be dropped and the linear equation remaining is the dipole version [27] of the Balitsky-Fadin-Kuraev-Lipatov (BFKL) equation [3, 4] whose solution is known in the saddle-point approximation [27]. In the high-energy regime where unitarity corrections become important or $S(\underline{x}_{ij}, Y)$ is small, eq. (3.4) is easier to use since the quadratic term $S(\underline{x}_{02}, Y)S(\underline{x}_{12}, Y)$ can be neglected. The solution in this region is also known [22, 29]. Also the transition region from the weak to the saturation regime (sometimes also called the "scaling region") has been explored; analytic expressions for the rapidity dependence of the saturation momentum and for the scattering amplitude have been extracted by the authors of Ref. [16] by solving the BFKL equation in the presence of a saturation boundary. These results have been recently confirmed by Munier and Peschanki [21] who have directly solved the Kovchegov equation in the scaling region. In the next section, we show these results and discuss their validity.

3.2 Solution to the Kovchegov equation

In the vicinity of the saturation regime, the amplitude for dipole-dipole scattering in laboratory frame emerging from the Kovchegov equation [21] or, equivalently, from the BFKL evolution in the presence of a saturation boundary [16], is[3]

$$T(x, x', Y) = \frac{4\sqrt{\pi}\alpha^2 x^2}{\lambda_0^2(1-\lambda_0)^2} \left[Q_c^2(Y)\, x'^2\right]^{1-\lambda_0} \Delta \left[\ln \frac{1}{Q_c^2(Y)\, x'^2} + \Delta\right] \times \exp\left[-\frac{\pi \ln^2(1/Q_c^2(Y)\, x'^2)}{4\alpha N_c \chi''(\lambda_0) Y}\right] . \quad (3.6)$$

Here all the values for the constants and the notations are adopted from Ref. [16]. The above amplitude results from the scattering amplitude (2.9) when evaluated in the vicinity of the boundary line $Q_c(Y)$, as done in [16], where

$$Q_c^2(Y)\; x^2 = \frac{\exp\left[\frac{2\alpha N_c}{\pi} \frac{\chi(\lambda_0)}{1-\lambda_0} Y\right]}{\left[\frac{4\alpha N_c}{\pi} \chi''(\lambda_0) Y\right]^{\frac{3}{2(1-\lambda_0)}}} \quad (3.7)$$

with $\lambda_0 = 0.372$ determined by

$$(1-\lambda_0)\chi'(\lambda_0) + \chi(\lambda_0) = 0 . \quad (3.8)$$

Up to a constant factor, $Q_c(Y)$ equals the saturation momentum $Q_s(Y)$, which separates the saturation regime from the weak scattering region. In Fig.4a we show

[3]The scattering amplitude shown here follows from eq.(4.1) of Ref. [16] in the vicinity of the saturation boundary, including the exponential function, which was neglected in eq.(4.2) there.

the line $Q_c(Y)$ in the $\ln x^2/z^2 - Y$ plane where z is generic; BFKL evolution takes place on the right-hand side of the line. All paths going into the saturation region on the left-hand side of the line are excluded.

The scattering amplitude (3.6) is valid in the region

$$\Delta \leq \ln \frac{1}{Q_c^2(Y)\, x'^2} \ll \sqrt{4\alpha N_c \chi''(\lambda_0) Y/\pi}\ , \tag{3.9}$$

and Δ is an irrelevant small constant depending on the fixed coupling α.

In the vicinity of the saturation boundary, i.e., for x'^2 close to $1/Q_c^2(Y)$, the scattering amplitude in (3.6) shows a scaling behaviour since it depends only on $Q_c^2(y)\, x'^2$; lines with constant $Q_c^2(y)\, x'^2$ are lines of constant scattering amplitude.

Expression (3.6) can be viewed as follows; one takes a dipole of size x at zero rapidity, evolves it to many smaller dipoles (their size is of order $1/Q_c(Y)$) as the rapidity increases up to Y, and scatters then these dipoles on an elementary dipole of size x'. This is shown in Fig. 4a. Equivalently, one may view the BFKL evolution also in the opposite direction, as shown in Fig. 4b, in which case the small dipole x' evolves to larger dipoles (size of order $1/\tilde{Q}_c(Y)$) which then scatter on the elementary dipole x. In this case the scattering amplitude takes the form

$$T(x', x, Y) = \frac{4\sqrt{\pi}\alpha^2 x^2}{\lambda_0^2(1-\lambda_0)^2} \left[\frac{1}{\tilde{Q}_c^2(Y)\, x^2}\right]^{1-\lambda_0} \Delta\left[\ln \tilde{Q}_c^2(Y)\, x^2 + \Delta\right] \times \exp\left[-\frac{\pi \ln^2(\tilde{Q}_c^2(Y)\, x^2)}{4\alpha N_c \chi''(\lambda_0) Y}\right]\ , \tag{3.10}$$

where $\tilde{Q}_c^2(Y)$ is defined by

$$Q_c^2(Y)\, x'^2 = \frac{1}{\tilde{Q}_c^2(Y)\, x^2}\ , \tag{3.11}$$

which is obvious from Figs. 4a and 4b. This additional way of viewing the scattering of two dipoles turns out to be useful in our further discussion, as we will see.

It is also useful to show the expressions for the dipole number densities in the vicinity of the saturation boundary. They are calcuated in the same way as the scattering amplitudes. The dipole number density for $x > x'$ reads

$$n(x, x', Y) = \frac{8}{\sqrt{\pi}} \left(\frac{x^2}{x'^2}\right) \left[Q_c^2(Y)\, x'^2\right]^{1-\lambda_0} \Delta\left[\ln \frac{1}{Q_c^2(Y)\, x'^2} + \Delta\right] \exp\left[-\frac{\pi \ln^2(1/Q_c^2(Y) x'^2)}{4\alpha N_c \chi''(\lambda_0) Y}\right] \tag{3.12}$$

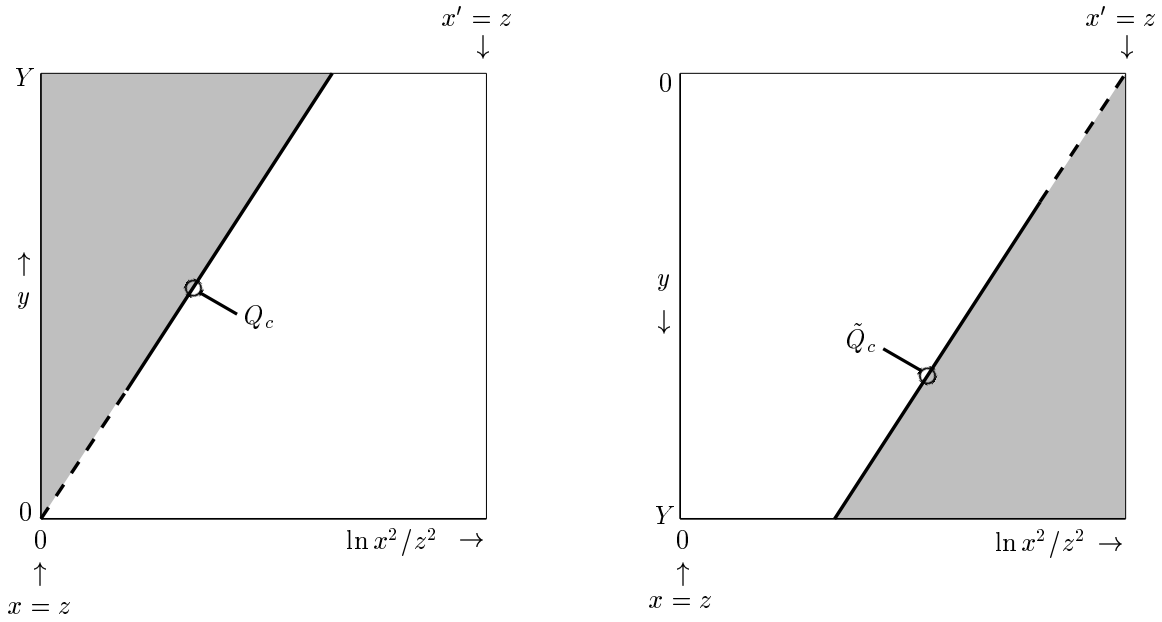

Figure 4: The saturation boundaries Q_c and $\tilde{Q}_c$ separate the saturated regime (shaded areas) from the weak interaction region. In (a) dipole x evolves from $y = 0$ up to $y = Y$ and scatters on the elementary dipole x' while in (b) dipole x' evolves from $y = 0$ up to $y = Y$ and scatters on the elementary dipole x.

and it is related to the scattering amplitude as

$$T(x, x', Y) = \frac{\pi}{2}\alpha^2 x'^2 \frac{1}{\lambda_0^2(1-\lambda_0)^2}\; n(x, x', Y)\;, \tag{3.13}$$

which is obvious from eqs. (2.3), (2.9) and (3.6). Eq. (3.13) explicitly shows that the elementary dipole x' scatters on the evolved dipoles x.

Similary, for the evolution from x' to x (with $x' < x$), one obtains

$$n(x', x, Y) = \frac{8}{\sqrt{\pi}}\left[\frac{1}{\tilde{Q}_c^2(Y)\, x^2}\right]^{1-\lambda_0} \Delta\left[\ln \tilde{Q}_c^2(Y)\, x^2 + \Delta\right] \exp\left[-\frac{\pi \ln^2(\tilde{Q}_c^2(Y)\, x^2)}{4\alpha N_c \chi''(\lambda_0) Y}\right]\;, \tag{3.14}$$

and has the relation

$$T(x', x, Y) = \frac{\pi}{2}\alpha^2 x^2 \frac{1}{\lambda_0^2(1-\lambda_0)^2}\; n(x', x, Y)\;, \tag{3.15}$$

as can be seen from (2.4), (2.9) and (3.10). As compared to (3.13), eq. (3.15) shows that the elementary dipole x scatters on the evolved dipole x'.

3.3 Completeness relation

3.3.1 Internal saturation boundaries

In this section we show that the scattering amplitude in the laboratory frame (3.6) resulting from the Kovchegov equation (or the BFKL evolution with a saturation boundary) is not consistent with the completeness relation. This becomes obvious if one tries to reproduce the result (3.6) by dividing the BFKL evolution in two successive steps in rapidity, say from $y = 0$ to $y = Y/2$ and then from $y = Y/2$ to $y = Y$ as shown in Fig. 5. To do this, we start with the scattering amplitude of two dipoles in the center-of-mass frame which is given by (2.1) with $y = Y/2$

$$T(x, x', Y) = \int \frac{d^2r_1 d^2r_2}{4\pi^2 r_1^2 r_2^2}\; n(x, r_1, Y/2)\; n(x', r_2, Y/2)\; \sigma_{dd}(r_1, r_2)\;. \tag{3.16}$$

Upon inserting the dipole number density (2.3), where $x > r_1$, and the dipole-dipole cross section (2.2) in (3.16), the integration over r_1 can be carried out as in (2.8), and the amplitude becomes

$$T(x, x', Y) = \pi\alpha^2 \int \frac{d^2r_2}{2\pi} \int \frac{d\lambda}{2\pi i}\; \frac{1}{\lambda^2(1-\lambda)^2} \exp\left[\frac{2\alpha N_c}{\pi}\chi(\lambda)\frac{Y}{2} - (1-\lambda)\ln\frac{x^2}{r_2^2}\right]\left(\frac{x^2}{r_2^2}\right) \times\; n(x', r_2, Y/2)\;. \tag{3.17}$$

Using relation (2.5) for $x' < r_2$, one can rewrite the amplitude as

$$T(x, x', Y) = \pi\alpha^2 x'^2 \int \frac{d^2r_2}{2\pi r_2^2} \int \frac{d\lambda}{2\pi i}\; \frac{1}{\lambda^2(1-\lambda)^2} \exp\left[\frac{2\alpha N_c}{\pi}\chi(\lambda)\frac{Y}{2} - (1-\lambda)\ln\frac{x^2}{r_2^2}\right]\left(\frac{x^2}{r_2^2}\right) \times\; n(r_2, x', Y/2) \tag{3.18}$$

which further can be expressed in terms of dipole number densities (cf. eq. (2.3)),

$$T(x, x', Y) = \frac{\pi}{2}\alpha^2 x'^2 \frac{1}{\lambda_0^2(1-\lambda_0)^2} \int \frac{d^2r_2}{2\pi r_2^2}\; n(x, r_2, Y/2)\; n(r_2, x', Y/2)\;. \tag{3.19}$$

It is at this point that we can identify the completeness relation. Requiring this expression to be the same as the result for the scattering amplitude in the laboratory frame (3.6), or equivalently (3.10), means that the following completeness relation,

$$n(x, x', Y) = \int \frac{d^2r_2}{2\pi r_2^2}\; n(x, r_2, Y/2)\; n(r_2, x', Y/2)\;, \tag{3.20}$$

has to be satisfied for the dipole number densities n evaluated in the presence of saturation boundaries. We note in passing that one can use eq. (2.3) to show that

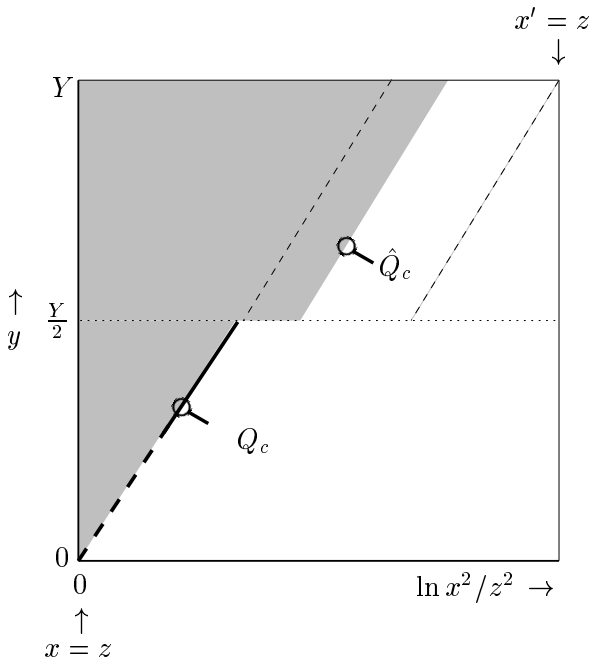

Figure 5: BFKL evolution in two successive steps $0 \to Y/2 \to Y$ in the presence of the internal saturation boundaries Q_c and $\hat{Q}_c$.

the naive BFKL evolution without saturation boundaries fulfilles the completeness relation.

Let us now check if the right-hand side (rhs) of (3.20) equals the left-hand side which is given by eq. (3.12). Inserting the dipole number density (3.12) with $Y \to Y/2$ in (3.20), the right-hand side becomes

$$
\begin{aligned}
[\text{rhs of (3.20)}] \;\; = \;\; & \frac{64}{\pi} \int \frac{d^2 r_2}{2\pi r_2^2} \qquad (3.21) \\
& \times \left(\frac{x^2}{r_2^2}\right) \left[Q_c^2(Y/2)\, r_2^2\right]^{1-\lambda_0} \Delta \left[\ln \frac{1}{Q_c^2(Y/2)\, r_2^2} + \Delta\right] \exp\left[-\frac{\pi \ln^2(1/Q_c^2(Y/2) r_2^2)}{4\alpha N_c \chi''(\lambda_0) Y/2}\right] \\
& \times \left(\frac{r_2^2}{x'^2}\right) \left[\hat{Q}_c^2(Y/2)\, x'^2\right]^{1-\lambda_0} \Delta \left[\ln \frac{1}{\hat{Q}_c^2(Y/2)\, x'^2} + \Delta\right] \exp\left[-\frac{\pi \ln^2(1/\hat{Q}_c^2(Y/2) x'^2)}{4\alpha N_c \chi''(\lambda_0) Y/2}\right],
\end{aligned}
$$

where $Q_c^2(Y/2)$ follows from (3.7) with Y replaced by $Y/2$, and $\hat{Q}_c^2(Y/2)$ is determined by matching the evolution at $Y/2$ (see Fig. 5),

$$
\hat{Q}_c^2(Y/2)\, r_2^2 = Q_c^2(Y/2)\, x^2 \; . \qquad (3.22)
$$

In equation (3.21) the second line gives the evolution of dipole x from $y = 0$ up to $y = Y/2$ and the third line gives the evolution of dipole r_2 from $Y/2$ up to Y. It is

important to note that while the evolution of dipole x is limited by the saturation boundary Q_c, the evolution of dipole r_2 is limited by its *own* (or *internal*) saturation boundary $\hat{Q}_c$ as shown by the two shaded areas in Fig. 5 in order to respect unitarity.

Using the matching (3.22) which gives

$$\begin{aligned}\left[Q_c^2(Y/2)\, r_2^2\right]^{1-\lambda_0}\left[\hat{Q}_c^2(Y/2)\, x'^2\right]^{1-\lambda_0} &= \left[Q_c^4(Y/2)x^2x'^2\right]^{1-\lambda_0} \\ &= \left[Q_c^2(Y)x'^2\right]^{1-\lambda_0}\frac{1}{\left[\frac{\alpha N_c}{\pi}\chi''(\lambda_0)Y\right]^{\frac{3}{2}}}\ , \quad (3.23)\end{aligned}$$

and the definitions

$$\eta = \ln\frac{1}{Q_c^2(Y/2)\, r_2^2}\ , \quad \zeta = \ln\frac{1}{Q_c^4(Y/2)x^2x'^2}\ , \quad \tau = \frac{\alpha N_c}{\pi}\chi''(\lambda_0)Y\ , \qquad (3.24)$$

equation (3.21) becomes

$$\begin{aligned}[\text{rhs of (3.20)}] &= \frac{8}{\pi}\left(\frac{x^2}{x'^2}\right)\left[Q_c^2(Y)\, x'^2\right]^{1-\lambda_0}\frac{1}{\tau^{\frac{3}{2}}}\int_{-\Delta}^{\zeta+\Delta} d\eta \qquad (3.25)\\ &\quad \times\Delta\left[\eta+\Delta\right]\exp\left[-\frac{\eta^2}{2\tau}\right]\Delta\left[\zeta-\eta+\Delta\right]\exp\left[-\frac{(\zeta-\eta)^2}{2\tau}\right]\ .\end{aligned}$$

The limits in the intgration over η follow from the positive definite dipole number densities (3.9). The integration over η is easily done and the result is

$$\begin{aligned}[\text{rhs of (3.20)}] &= \frac{8}{\pi}\left(\frac{x^2}{x'^2}\right)\left[Q_c^2(Y)\, x'^2\right]^{1-\lambda_0}\frac{1}{\tau^{\frac{3}{2}}}\frac{\Delta^2}{8}(2\tau)\exp\left[\frac{3\zeta^2+6\zeta\Delta+4\Delta^2}{2\tau}\right]\\ &\times\left[2(\zeta+2\Delta)\exp\left[\frac{(\zeta+\Delta)^2}{\tau}\right]+\left((\zeta+2\Delta)^2-2\tau\right)\exp\left[\frac{5\zeta^2+12\zeta\Delta+8\Delta^2}{4\tau}\right]\sqrt{\frac{\pi}{\tau}}\,\mathrm{Erf}\left[\frac{\zeta+2\Delta}{\sqrt{4\tau}}\right]\right]. \qquad (3.26)\end{aligned}$$

Inserting this expression in (3.19), one obtains for the scattering amplitude

$$\begin{aligned}T(x,x',Y) &= \frac{\alpha^2x^2}{\lambda_0^2(1-\lambda_0)^2}\left[Q_c^2(Y)\, x'^2\right]^{1-\lambda_0}\frac{\Delta^2}{\tau^{\frac{1}{2}}}\exp\left[\frac{3\zeta^2+6\zeta\Delta+4\Delta^2}{2\tau}\right]\\ &\times\left[2(\zeta+2\Delta)\exp\left[\frac{(\zeta+\Delta)^2}{\tau}\right]+\left((\zeta+2\Delta)^2-2\tau\right)\exp\left[\frac{5\zeta^2+12\zeta\Delta+8\Delta^2}{4\tau}\right]\sqrt{\frac{\pi}{\tau}}\,\mathrm{Erf}\left[\frac{\zeta+2\Delta}{\sqrt{4\tau}}\right]\right]. \qquad (3.27)\end{aligned}$$

This result is not the same as the result for the scattering amplitude in laboratory frame (3.6). Thus, the Kovchegov equation or, equivalently, the BFKL evolution in the presence of a saturation boundary does not satisfy the completeness relation.

3.3.2 Global saturation boundary

In this section we show that if the evolution of dipole r_2 from $Y/2$ to Y is limited by the saturation boundary Q_c as shown in Fig. 6, rather than $\hat{Q}_c$ as in the previous section, then the scattering amplitude resulting from the Kovchegov equation obeys the completeness relation. However, in this case the evolution of dipole r_2, for some values of r_2, violates unitarity, i.e. $T(r_2, x', Y/2) > 1$. To clarify this point, let's consider the two regions:

$r_2 < 1/\tilde{Q}_c(Y/2)$: The amplitude $T(r_2, x', Y/2)$ is always larger than 1 since any evolution path from r_2 to x' goes through the internal saturation region of dipole r_2 being on the lhs of $\hat{Q}_c$ as shown by the dashed-dotted line in Fig. 6.

$r_2 > 1/\tilde{Q}_c(Y/2)$: Each path of evolution from x to r_2 to x' respects unitarity. However, also in this region there are paths going from an intermediate point to another along which $T(r_2, x', Y/2)$ becomes larger than 1 due to the same reason as above. For example along the dashed-dotted-dotted line in Fig. 6.

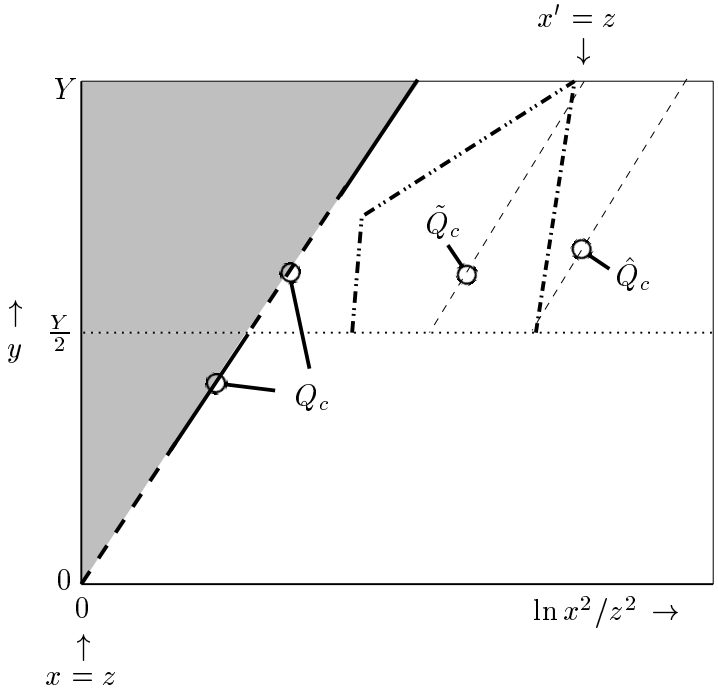

Figure 6: BFKL evolution in two successive steps $0 \to Y/2 \to Y$ in the presence of a global saturation boundary Q_c.

The successive evolution $0 \to Y/2$ and $Y/2 \to Y$ in the presence of a global

(fixed) saturation boundary Q_c as shown in Fig. 6 is given by

$$\begin{aligned}
[\text{rhs of (3.20)}] &= \frac{64}{\pi}\int\frac{d^2r_2}{2\pi r_2^2} \qquad (3.28)\\
&\times\left(\frac{x^2}{r_2^2}\right)\left[Q_c^2(Y/2)\,r_2^2\right]^{1-\lambda_0}\Delta\left[\ln\frac{1}{Q_c^2(Y/2)\,r_2^2}+\Delta\right]\exp\left[-\frac{\pi\ln^2(1/Q_c^2(Y/2)r_2^2)}{4\alpha N_c\chi''(\lambda_0)Y/2}\right]\\
&\times\left(\frac{r_2^2}{x'^2}\right)\left[\hat{Q}_c^2(Y/2)\,x'^2\right]^{1-\lambda_0}\left[\ln\left(\frac{Q_c^2(Y)r_2^2}{Q_c^2(Y/2)\,x^2}e^{-\Delta}\right)\ln\left(Q_c^2(Y)\,x'^2e^{-\Delta}\right)\right]\\
&\times\exp\left[-\frac{\pi\ln^2(1/\hat{Q}_c^2(Y/2)x'^2)}{4\alpha N_c\chi''(\lambda_0)Y/2}\right].
\end{aligned}$$

The last two lines (multiplied by $8/\sqrt{\pi}$) give the dipole number density $n(r_2,x',Y/2)$ which vanishes at $x'=e^{-\Delta}/Q_c$ or near the saturation boundary Q_c. To obtain this result, one evaluates $n(r_2,x',Y)$ in the vicinity of $\hat{Q}_c$ following [16] and requires it to vanish at $x'=e^{-\Delta}/Q_c(Y)$ (instead of $x'=e^{-\Delta}/\hat{Q}_c(Y)$) when saturation (eq.(4.1) of [16]) is taken into account. This requirement opens ways of evolution which violate unitarity as mentioned above. Note the difference between (3.28) and (3.21); in (3.21) $n(r_2,x,Y/2)$ vanishes at $x'=e^{-\Delta}/\hat{Q}_c$.

Using eq. (3.22) one gets

$$\ln\left(\frac{Q_c^2(Y)r_2^2}{Q_c^2(Y/2)\,x^2}e^{-\Delta}\right)=\ln(Q_c^2(Y/2)\,r_2^2)+\frac{3}{2(1-\lambda_c)}\ln\left[\frac{\alpha N_c}{\pi}\chi''(\lambda_c)Y\right]-\Delta \qquad (3.29)$$

and

$$\ln(1/\hat{Q}_c^2(Y/2)x'^2)=\ln(Q_c^2(Y/2)\,r_2^2)+\frac{3}{2(1-\lambda_c)}\ln\left[\frac{\alpha N_c}{\pi}\chi''(\lambda_c)Y\right]-\ln(Q_c^2(Y)\,x'^2) \qquad (3.30)$$

which allow us to evaluate eq. (3.28) in the vicinity of the saturation boundary $x'\approx 1/Q_c(Y)$ in the logarithmic approximation. Using in addition also eq.(3.23), we get

$$\begin{aligned}
[\text{rhs of (3.20)}] &= -\frac{8}{\pi}\left(\frac{x^2}{x'^2}\right)\left[Q_c^2(Y)x'^2\right]^{1-\lambda_0}\frac{1}{\left[\frac{\alpha N_c}{\pi}\chi''(\lambda_0)Y\right]^{\frac{3}{2}}}\ln\left(Q_c^2(Y)\,x'^2e^{-\Delta}\right)\\
&\times\int_0^\infty d\ln(Q_c^2(Y/2)\,r_2^2)\;\ln^3(Q_c^2(Y/2)\,r_2^2)\;\exp\left[-\frac{\pi\ln^2(Q_c^2(Y/2)r_2^2)}{\alpha N_c\chi''(\lambda_0)Y}\right] \qquad (3.31)
\end{aligned}$$

which after the integration over $\ln(Q_c^2(Y/2)\,r_2^2)$ gives

$$[\text{rhs of (3.20)}] = \frac{8}{\pi}\left(\frac{x^2}{x'^2}\right)\left[Q_c^2(Y)x'^2\right]^{1-\lambda_0}\Delta\left[\ln\frac{1}{Q_c^2(Y)\,x'^2}+\Delta\right]. \qquad (3.32)$$

This result agrees with the result for the left-hand side of the completeness relation given by (2.3) (the additional exponential function in (2.3) becomes one in the very vicinity of the saturation boundary which is considered here.). Note, however, that in order to satisfy completeness one had to violate unitarity.

3.4 Frame-dependence

In this section we show that the result for the scattering amplitude obtained in the laboratory frame (3.6) is frame-dependent. For simplicity, we consider here the scattering of two dipoles in the c.m. frame (see Fig. 7) and show that the result disagrees with the result for the scattering amplitude in the laboratory frame (3.6).

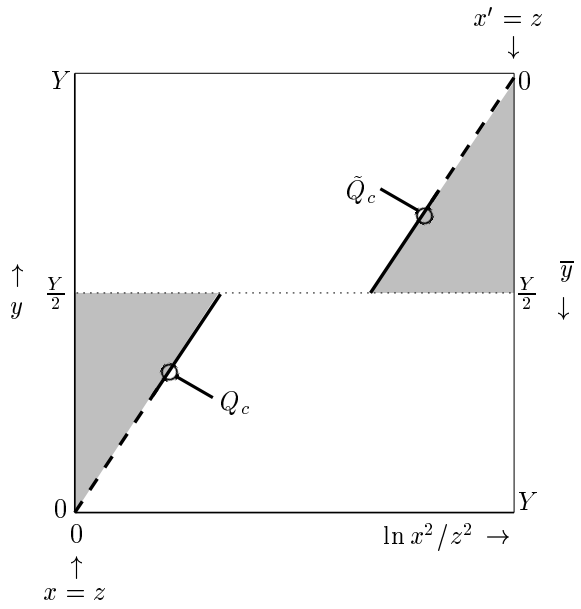

Figure 7: Dipole-dipole scattering in the presence of saturation (shaded area) in the center-of-mass frame.

The scattering amplitude of two dipoles in the c.m. frame is given by (3.16), or after the integration over r_1, by (2.9). With the dipole number densities (3.12) and (3.14), the scattering amplitude (2.9) becomes

$$T(x, x', Y) \;=\; \frac{\pi}{2}\alpha^2 \frac{1}{\lambda_0^2(1-\lambda_0)^2} \int \frac{d^2 r_2}{2\pi}$$

$$\times\frac{8}{\sqrt{\pi}}\left(\frac{x^2}{r_2^2}\right)\left[Q_c^2(Y/2)\,r_2^2\right]^{1-\lambda_0}\Delta\left[\ln\frac{1}{Q_c^2(Y/2)\,r_2^2}+\Delta\right]\exp\left[-\frac{\pi\ln^2(1/Q_c^2(Y/2)r_2^2)}{4\alpha N_c\chi''(\lambda_0)Y/2}\right]$$
$$\times\frac{8}{\sqrt{\pi}}\left[\frac{1}{\tilde{Q}_c^2(Y/2)\,r_2^2}\right]^{1-\lambda_0}\Delta\left[\ln\tilde{Q}_c^2(Y/2)\,r_2^2+\Delta\right]\exp\left[-\frac{\pi\ln^2(\tilde{Q}_c^2(Y/2)\,r_2^2)}{4\alpha N_c\chi''(\lambda_0)Y/2}\right]\ , \quad (3.33)$$

where $\tilde{Q}_c^2(Y/2)$ is given by (3.11). For the dipole of size x, the evolution proceeds from $y = 0$ up to $y = Y/2$, while for the dipole of size x' evolution goes from $\overline{y} \equiv Y - y = 0$ to $\overline{y} = Y/2$ as shown in Fig. 7 where the shaded saturation regions of the two dipoles are shown. With the definitions in (3.23), one can easily see that the above amplitude leads to the result (3.27) which differs from the result for the scattering amplitude in the laboratory frame (3.6).

4 BFKL evolution in the presence of saturation

In this section we solve the BFKL equation in the presence of two saturation boundaries, ρ_1 and ρ_2, as shown in Fig. 8. Consider the scattering process where dipole x evolves from $y = 0$ up to $y = Y$ and then scatters on the elementary dipole x'. In this frame, the boundary ρ_1 is due to parton saturation in the wavefunction of the evolved dipole x. The second boundary ρ_2 excludes all paths of evolution from any intermediate point $(\rho, 0 < y < Y)$ to the final point $(x',\ Y)$ with $\rho > \rho_2$ which manifestly violate unitarity as discussed for the case $r_2 < 1/\tilde{Q}_c(Y/2)$ in sec. 3.3.2. In other words, the second boundary ρ_2 ensures unitarity respecting amplitudes for each path of evolution from $(x,\ 0)$ to $(x',\ Y)$ when the evolution proceeds in two steps, from the initial point $(x,\ 0)$ to an intermediate point (ρ, y) with $\rho_1 < \rho < \rho_2$ and then from the intermediate point (ρ, y) to the final point $(x',\ Y)$. However, the second boundary does not eliminate unitarity violating amplitudes when the evolution proceeds through two or more intermediate stages; paths of evolution from an intermediate point to another may violate unitarity since they may enter the internal saturation regimes as explained in the case of $r_2 > 1/\tilde{Q}_c(Y/2)$ in sec. 3.3.2. To eliminate also this remaining unitarity violating evolution one has to solve the Balitsky [10] or JIMWLK [12, 13] equation which are difficult to deal with analytically. The introduction of the second boundary ρ_2 has another advantage: it makes the scattering amplitude boost-invariant which was not the case for a single saturation boundary. Thus, the calculation in the center of mass, say, now gives the same result as the calculation in the laboratory frame of one of the two dipoles.

We may view the scattering process also backwards, i.e., in a frame where the

evolved dipole x' scatters on the elementary dipole x. In this frame, the boundary ρ_2 is due to parton saturation in the wavefunction of the evolved dipole x' and ρ_1 excludes all paths of evolution going to x that manifestly violate unitarity.

4.1 Diffusion in the presence of two absorptive barriers

In this section we solve the diffusion equation in the presence of two absorptive barriers and use the solution to calculate the scattering amplitude in the following section.

Consider the diffusion equation

$$\frac{\partial}{\partial t}\psi(\rho,t) = \frac{1}{4}\frac{\partial^2}{\partial\rho^2}\psi(\rho,t) \tag{4.1}$$

with the boundary conditions

$$\psi(\rho_1,t) = \psi(\rho_2,t) = 0 \tag{4.2}$$

and the initial condition

$$\psi(\rho,0) = \delta(\rho-\tilde{\rho})\ . \tag{4.3}$$

This boundary-value problem can be solved by the method of separation of variables. Specifically, we will (a) find solutions $\psi_n(\rho,t) = f_n(\rho)g_n(t)$ of (4.1) and (4.2) and (b) find the general solution $\psi(\rho,t)$ satisfying also the initial condition (4.3) by taking a suitable linear combination of the functions $\psi_n(\rho,t)$.

(a) Inserting $\psi_n(\rho,t) = f_n(\rho)g_n(t)$ in (4.1), we obtain

$$f_n(\rho)g_n'(t) = \frac{1}{4}f_n''(\rho)g_n(t) \tag{4.4}$$

or

$$\frac{g_n'(t)}{g_n(t)/4} = \frac{f_n''(\rho)}{f_n(\rho)}\ . \tag{4.5}$$

Next, we observe that the left-hand side of (4.5) is a function of t alone, while the right-hand side is a function of ρ alone. This implies that

$$\frac{g_n'(t)}{g_n(t)/4} = \frac{f_n''(\rho)}{f_n(\rho)} = -\lambda_n \tag{4.6}$$

for some constant λ_n. In addition, the boundary conditions (4.2) imply that $f_n(\rho_1) = 0$ and $f_n(\rho_2) = 0$. Hence $\psi_n(\rho,t)$ is a solution of (4.1) if

$$f_n''(\rho) + \lambda_n f_n(\rho) = 0\ , \quad f_n(\rho_1) = f_n(\rho_2) = 0 \tag{4.7}$$

and

$$g_n''(t) + \frac{1}{4}\lambda_n g_n(t) = 0 \ . \tag{4.8}$$

The boundary-value problem (4.7) has a solution only if $\lambda_n = n^2\pi^2/(\rho_2 - \rho_1)^2$, and in this case,

$$f_n(\rho) = \sin\left(\frac{n\pi(\rho - \rho_1)}{\rho_2 - \rho_1}\right) \tag{4.9}$$

for every positive integer $n = 1, 2...$ and $\rho_1 < \rho < \rho_2$. Equation (4.8), in turn, implies that

$$g_n(t) = e^{-\frac{n^2\pi^2}{(\rho_2-\rho_1)^2}\frac{t}{4}} \ . \tag{4.10}$$

Hence,

$$\psi_n(\rho, t) = c_n \sin\left(\frac{n\pi(\rho - \rho_1)}{\rho_2 - \rho_1}\right) e^{-\frac{n^2\pi^2}{(\rho_2-\rho_1)^2}\frac{t}{4}} \tag{4.11}$$

for every constant c_n to be fixed by the initial condition (4.3).

(b) The linear combination

$$\psi(\rho, t) = \sum_{n=1}^{\infty} c_n \sin\left(\frac{n\pi(\rho - \rho_1)}{\rho_2 - \rho_1}\right) e^{-\frac{n^2\pi^2}{(\rho_2-\rho_1)^2}\frac{t}{4}} \tag{4.12}$$

satifies the boundary conditions (4.1). To satisfy the initial condition (4.3), we must choose the constants c_n such that

$$\psi(\rho, 0) = \sum_{n=1}^{\infty} c_n \sin\left(\frac{n\pi(\rho - \rho_1)}{\rho_2 - \rho_1}\right) = \delta(\rho - \tilde{\rho}) \ . \tag{4.13}$$

on the interval $\rho_1 < \rho, \tilde{\rho} < \rho_2$. Using Fourier analysis, the constants c_n are

$$c_n = \frac{2}{\rho_2 - \rho_1}\int_{\rho_1}^{\rho_2} d\rho \ \delta(\rho - \tilde{\rho}) \sin\left(\frac{n\pi(\rho - \rho_1)}{\rho_2 - \rho_1}\right) = \frac{2}{\rho_2 - \rho_1}\sin\left(\frac{n\pi(\tilde{\rho} - \rho_1)}{\rho_2 - \rho_1}\right) \ . \tag{4.14}$$

Thus,

$$\psi(\rho, t) = \sum_{n=1}^{\infty} \frac{2}{\rho_2 - \rho_1}\sin\left(\frac{n\pi(\tilde{\rho} - \rho_1)}{\rho_2 - \rho_1}\right) \sin\left(\frac{n\pi(\rho - \rho_1)}{\rho_2 - \rho_1}\right) e^{-\frac{n^2\pi^2}{(\rho_2-\rho_1)^2}\frac{t}{4}} \tag{4.15}$$

is the general solution.

4.2 BFKL evolution between two saturation boundaries

Here we wish to evaluate the scattering amplitude in the laboratory frame (2.9) in the region between the weak and the saturation regimes in analogy to Ref. [16]. Hence, we define a particular line $Q_d^2(Y)$ in the $\ln(x^2/x'^2) - Y$ plane by the two conditions

$$\frac{2\alpha N_c}{\pi}\chi'(\lambda_d)Y + \ln(Q_d^2\, x^2) = 0 \tag{4.16}$$

and

$$\frac{2\alpha N_c}{\pi}\chi(\lambda_d)Y - (1-\lambda_d)\ln(Q_d^2\, x^2) = \frac{\pi^2}{(\rho_2-\rho_1)^2}\frac{\alpha N_c}{\pi}\chi''(\lambda_d)Y\ . \tag{4.17}$$

Eq. (4.16) is the saddle-point condition while eq. (4.17) is chosen so that the scattering amplitude becomes a constant along the line $Q_d(Y)$, as we will see. ρ_2 and ρ_1 denote the two boundaries limiting the BFKL evolution as shown in Fig. 8. The solution to (4.16) and (4.17) is

$$(1-\lambda_d)\chi'(\lambda_d) + \chi(\lambda_d) = \frac{\pi^2}{2(\rho_2-\rho_1)^2}\chi''(\lambda_d) \tag{4.18}$$

and

$$Q_d^2(Y)\, x^2 = \exp\left[\frac{2\alpha N_c}{\pi}\frac{\chi(\lambda_d)}{1-\lambda_d}Y\left(1 - \frac{\pi^2}{2(\rho_2-\rho_1)^2}\frac{\chi''(\lambda_d)}{\chi(\lambda_d)}\right)\right]. \tag{4.19}$$

Eq. (4.18) determines λ_d which is a constant for fixed Y, x and x' or fixed $\rho_2 - \rho_1$. For large $\rho_2 - \rho_1$, λ_d approaches $\lambda_0 = 0.372$ which is given by (3.8) since

$$\lambda_d - \lambda_0 = \frac{\pi^2}{2(\rho_2-\rho_1)^2}\frac{1}{1-\lambda_0}\ . \tag{4.20}$$

Now we evaluate the scattering amplitude (2.9) in a region around $Q_d^2(Y)$ by the saddle-point method, when αY is large. This means that we expand the exponent in (2.9) around λ_d (since λ_d satisfies the saddle-point condition) and then use (4.16) and (4.17). One obtains

$$\begin{aligned} T(x,x',Y) \;&=\; \frac{\pi\alpha^2 x^2}{\lambda_d^2(1-\lambda_d)^2}\left(Q_d^2(Y)\, x'^2\right)^{1-\lambda_d}\exp\left[\frac{\pi^2}{(\rho_2-\rho_1)^2}\frac{\alpha N_c}{\pi}\chi''(\lambda_d)Y\right] \\ &\quad\times\int\frac{d\lambda}{2\pi i}\exp\left[\frac{\alpha N_c}{\pi}\chi''(\lambda_d)Y(\lambda-\lambda_d)^2 + (\lambda-\lambda_d)\ln\frac{1}{Q_d^2(Y)\, x'^2}\right] \end{aligned} \tag{4.21}$$

After the simple Gaussian integral, the amplitude becomes

$$\begin{aligned} T(x,x',Y) \;&=\; \frac{\pi\alpha^2 x^2}{\lambda_d^2(1-\lambda_d)^2}\left(Q_d^2(Y)\, x'^2\right)^{1-\lambda_d}\exp\left[\frac{\pi^2}{(\rho_2-\rho_1)^2}\frac{\alpha N_c}{\pi}\chi''(\lambda_d)Y\right] \\ &\quad\times\frac{1}{\sqrt{4\alpha N_c\chi''(\lambda_d)Y}}\ \exp\left[-\frac{\pi\ln^2(1/Q_d^2(Y)\, x'^2)}{4\alpha N_c\chi''(\lambda_d)Y}\right]\ . \end{aligned} \tag{4.22}$$

To simplify notations, we use

$$\rho = \ln\left(\frac{x^2}{x'^2}\right), \quad \rho_d(Y) = \ln(Q_d^2(Y)\, x^2), \quad t = \frac{4\alpha N_c \chi''(\lambda_d) Y}{\pi} \tag{4.23}$$

and

$$\psi(\rho - \rho_d, t) = \frac{1}{\sqrt{\pi t}} e^{-\frac{(\rho-\rho_d)^2}{t}} \ . \tag{4.24}$$

In terms of the above the amplitude becomes

$$T(x, x', Y) = \frac{\pi \alpha^2 x^2}{\lambda_d^2 (1-\lambda_d)^2} e^{-(1-\lambda_d)(\rho-\rho_d)} \ \exp\left[\frac{\pi^2}{(\rho_2-\rho_1)^2}\frac{t}{4}\right] \ \psi(\rho - \rho_d, t) \ . \tag{4.25}$$

Here the function $\psi(\rho - \rho_d, t)$ represents the diffusive part of the amplitude since it satisfies the diffusion equation

$$\frac{\partial}{\partial t}\psi(\rho - \rho_d, t) = \frac{1}{4}\frac{\partial^2}{\partial \rho^2}\psi(\rho - \rho_d, t) \ . \tag{4.26}$$

Eq.(4.24) is not the proper solution of the diffusion equation (4.26) in the presence of saturation. It is at this point that we impose the unitarity. To obtain the right solution in the presence of saturation, one has to exclude paths which go into the saturation region while solving (4.26). This can be realized by requiring $\psi(\rho - \rho_d, t)$ to vanish at the saturation boundaries. A solution to the diffusion equation with two saturation boundary conditions is presented in Sec. 4.1. The general solution for $\psi(\rho - \rho_d, t)$ in the presence of saturation is given by (4.15). However, to simplify calculations, we will consider the scattering ampitude at large rapidities,

$$t \gg \frac{4(\rho_2 - \rho_1)^2}{\pi^2} \ , \tag{4.27}$$

where the function $\psi(\rho - \rho_d, t)$ in (4.15) is dominated by the lowest mode $n = 1$,

$$\psi_s(\rho, t) = \frac{2}{\rho_2 - \rho_1} \sin\left(\frac{\pi(\tilde{\rho} - \rho_1(0))}{\rho_2 - \rho_1}\right) \sin\left(\frac{\pi(\rho - \rho_1)}{\rho_2 - \rho_1}\right) e^{-\frac{\pi^2}{(\rho_2-\rho_1)^2}\frac{t}{4}} \ . \tag{4.28}$$

Note that $\rho_1 < \rho < \rho_2$ (cf. Fig. 8), $\psi_s(\rho_1, t) = \psi_s(\rho_2, t) = 0$, and $\tilde{\rho}$ is a parameter which fixes the initial condition (4.3); we choose $\tilde{\rho} = 0$ at $t = 0$.

With (4.28) the scattering amplitude (4.25) now becomes

$$T(x, x', Y) = \frac{\pi \alpha^2 x^2}{\lambda_d^2 (1-\lambda_d)^2} \frac{2}{\rho_2 - \rho_1} e^{-(1-\lambda_d)(\rho - \rho_d(Y))} \sin\left(\frac{\pi(\tilde{\rho}(0) - \rho_1(0))}{\rho_2 - \rho_1}\right) \sin\left(\frac{\pi(\rho - \rho_1(Y))}{\rho_2 - \rho_1}\right). \tag{4.29}$$

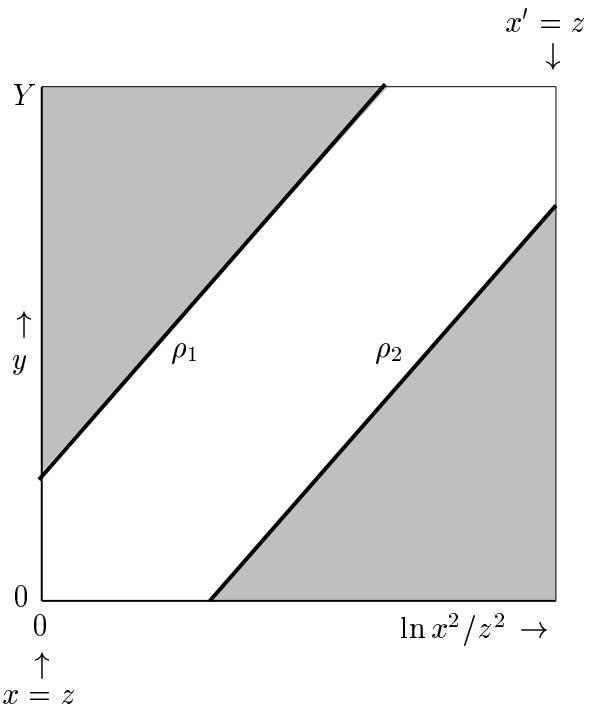

Figure 8: BFKL evolution between two shaded saturation regimes.

In order to fix ρ_2 and ρ_1, we consider the amplitudes $T(x,z,y)$ and $T(x',z,y)$ with $x > z > x'$ and $0 < y < Y$. $T(x,z,y)$ follows from (4.29) with ρ replaced by $\rho' = \ln(x^2/z^2)$ and Y by y,

$$T(x,z,y) = \frac{\pi\alpha^2 x^2}{\lambda_d^2(1-\lambda_d)^2}\frac{2}{\rho_2-\rho_1}e^{-(1-\lambda_d)(\rho'-\rho_d(y))}\sin\left(\frac{\pi(\tilde{\rho}(0)-\rho_1(0))}{\rho_2-\rho_1}\right)\sin\left(\frac{\pi(\rho'-\rho_1(y))}{\rho_2-\rho_1}\right). \tag{4.30}$$

$T(x',z,y)$ can also be easily obtained; one starts with (2.9), uses $\ln(1/\tilde{Q}_d^2(Y)\,x'^2)$ instead of $\ln(Q_d^2(Y)\,x^2)$ in eqs. (4.16) and (4.17), and follows otherwise the steps needed to compute the scattering amplitude in (4.29). Following this way, one gets

$$\begin{aligned} T(x',z,y) &= \frac{\pi\alpha^2 x^2}{\lambda_d^2(1-\lambda_d)^2}\frac{2}{\rho_2-\rho_1}e^{(1-\lambda_d)(\rho'-\tilde{\rho}_d(y))} \\ &\quad\times\sin\left(\frac{\pi(\rho_2(Y)-\ln(x^2/x'^2))}{\rho_2-\rho_1}\right)\sin\left(\frac{\pi(\rho_2(y)-\rho')}{\rho_2-\rho_1}\right) \end{aligned} \tag{4.31}$$

with

$$\tilde{\rho}_d(y) = \ln\left(\frac{x^2}{x'^2}\right) - \frac{2\alpha N_c}{\pi}\frac{\chi(\lambda_d)}{1-\lambda_d}\left(1-\frac{\pi^2}{2(\rho_2-\rho_1)^2}\frac{\chi''(\lambda_d)}{\chi(\lambda_d)}\right)(Y-y). \tag{4.32}$$

The amplitude $T(x,z,y)$ becomes maximum,

$$\frac{\partial}{\partial\rho'}T(x,z,y)\Big|_{\rho_{is}} = 0 \ , \tag{4.33}$$

at the saturation boundary,

$$\rho_{is}(y) = \rho_1(y) + \frac{1}{1-\lambda_d} \ . \tag{4.34}$$

We emphasize that here ρ_{is} is the saturation line for internal evolution once x, x' and Y have been fixed. It is not the saturation line for our overall scattering matrix $T(x,x',Y)$. We determine $\rho_1(y)$ by setting the amplitude at ρ_{is}

$$T(\rho'=\rho_{is},y) = 2\pi x^2 c, \tag{4.35}$$

with c a constant of order 1 as required by unitarity. Eqs. (4.34) and (4.35) give

$$\rho_1(y)=\frac{2\alpha N_c}{\pi}\frac{\chi(\lambda_d)}{1-\lambda_d}\left[1-\frac{\pi^2}{2(\rho_2-\rho_1)^2}\frac{\chi''(\lambda_d)}{\chi(\lambda_d)}\right]y-\frac{1}{1-\lambda_d}\ln\left[\frac{c\lambda_d^2(1-\lambda_d)^3(\rho_2-\rho_1)^2e}{\pi\alpha^2\sin\left(-\pi\rho_1(0)/(\rho_2-\rho_1)\right)}\right]. \tag{4.36}$$

Using $T(x',z,y)$ given by (4.31) instead of $T(x,z,y)$, one analogously obtains

$$\tilde{\rho}_{is}(y) = \rho_2(y) - \frac{1}{1-\lambda_d} \tag{4.37}$$

and

$$\begin{aligned}\rho_2(y) = \ln\left(\frac{x^2}{x'^2}\right) \ &+ \ \frac{1}{1-\lambda_d}\ln\left[\frac{c\lambda_d^2(1-\lambda_d)^3(\rho_2-\rho_1)^2e}{\pi\alpha^2\sin\left(\frac{\pi(\rho_2(Y)-\ln(x^2/x'^2))}{\rho_2-\rho_1}\right)}\right] \\ &- \ \frac{2\alpha N_c}{\pi}\frac{\chi(\lambda_d)}{1-\lambda_d}\left[1-\frac{\pi^2}{2(\rho_2-\rho_1)^2}\frac{\chi''(\lambda_d)}{\chi(\lambda_d)}\right](Y-y) \ .\end{aligned} \tag{4.38}$$

Thus,

$$\begin{aligned}\rho_2-\rho_1 = \ln\left(\frac{x^2}{x'^2}\right) \ &- \ \frac{2\alpha N_c}{\pi}\frac{\chi(\lambda_d)}{1-\lambda_d}\left[1-\frac{\pi^2}{2(\rho_2-\rho_1)^2}\frac{\chi''(\lambda_d)}{\chi(\lambda_d)}\right]Y \\ &+ \ \frac{2}{1-\lambda_d}\ln\left[\frac{c\lambda_d^2(1-\lambda_d)^3(\rho_2-\rho_1)^2e}{\pi\alpha^2\sin\left(-\pi\rho_1(0)/(\rho_2-\rho_1)\right)}\right]\end{aligned} \tag{4.39}$$

or in terms of the saturation line

$$\rho_2-\rho_1 = \ln\left(\frac{x^2}{x'^2}\right) - \rho_{is}(Y) + \frac{1}{1-\lambda_d}\ln\left[\frac{c\lambda_d^2(1-\lambda_d)^3(\rho_2-\rho_1)^2e^2}{\pi\alpha^2\sin\left(-\pi\rho_1(0)/(\rho_2-\rho_1)\right)}\right] \tag{4.40}$$

with

$$\rho_{is}(Y) = \frac{2\alpha N_c}{\pi}\frac{\chi(\lambda_d)}{1-\lambda_d}\left[1-\frac{\pi^2}{2(\rho_2-\rho_1)^2}\frac{\chi''(\lambda_d)}{\chi(\lambda_d)}\right]Y+\frac{2}{1-\lambda_d} -\frac{1}{1-\lambda_d}\ln\left[\frac{c\lambda_d^2(1-\lambda_d)^3(\rho_2-\rho_1)^2e^2}{\pi\alpha^2\sin\left(-\pi\rho_1(0)/(\rho_2-\rho_1)\right)}\right] . \quad (4.41)$$

The above quantities ρ_1, ρ_2, $\rho_2-\rho_1$, and ρ_{is} are determined once the dipole sizes x and x' and their relative rapidity Y are known.

The distance $\rho_2-\rho_1$ becomes minimum in the region $\ln(x^2/x'^2)\geq\rho_{is}(Y)$ exactly at $\ln(x^2/x'^2)=\rho_{is}(Y)$ or $x'=1/Q_{is}(Y)$, in which case (4.40) reduces to

$$\Delta\rho=\frac{1}{1-\hat{\lambda}_d}\ln\left[\frac{c\hat{\lambda}_d^2(1-\hat{\lambda}_d)^3(\Delta\rho)^2e^2}{\pi\alpha^2\sin\left(-\pi\hat{\rho}_1(0)/\Delta\rho\right)}\right] \quad (4.42)$$

where $\Delta\rho$ denotes the minimum of $\rho_2-\rho_1$ while $\hat{\lambda}_d$ and $\hat{\rho}_1(0)$ follow from (4.18) and (4.36) with $\rho_2-\rho_1$ replaced by $\Delta\rho$. Comparing (4.36) with (4.42), we have

$$-\hat{\rho}_1(0)=\Delta\rho-\frac{1}{1-\hat{\lambda}_d} \quad (4.43)$$

which when inserted in (4.42) leads to

$$\Delta\rho=\frac{1}{1-\hat{\lambda}_d}\ln\left[\frac{c\hat{\lambda}_d^2(1-\hat{\lambda}_d)^4(\Delta\rho)^3e^2}{\pi^2\alpha^2}\right] . \quad (4.44)$$

This equation can be solved by iteration, for small α, and the solution is

$$\Delta\rho(\alpha)=\frac{2}{1-\lambda_0}\ln\frac{1}{\alpha}+\frac{3}{1-\lambda_0}\ln\ln\frac{1}{\alpha}+\mathcal{O}(\text{const.}) . \quad (4.45)$$

The scaling behavior of T, as given in (4.29), and even the value of the saturation momentum is rather subtle. At first glance it appears that (4.29) would give an exponential behavior in ρ, a behavior identical to the scaling behavior known to follow from the Kovchegov equation. However, this is not the case because $\rho_d(Y)$ has a strong ρ-dependence also. To investigate further the ρ-dependence of T define

$$\frac{d\rho_d(Y)}{d\rho}\equiv\zeta \quad (4.46)$$

where the ρ and Y dependence of ζ is to be determined. Differentiating (4.16) with respect to ρ gives

$$\frac{d\lambda_d}{d\rho}=\frac{-\zeta}{2\alpha N_c\chi''(\lambda_d)Y/\pi}\approx\frac{-\zeta}{2\alpha N_c\chi''(\lambda_0)Y/\pi} \quad (4.47)$$

while differentiating (4.20) gives

$$\frac{d\lambda_d}{d\rho} = -\frac{\pi^2}{(1-\lambda_0)(\rho_2-\rho_1)^3}\frac{d(\rho_2-\rho_1)}{d\rho} \ . \tag{4.48}$$

Equating the right hand side of (4.47) and (4.48) leads to

$$\frac{d(\rho_2-\rho_1)}{d\rho} = \frac{\zeta(1-\lambda_0)(\rho_2-\rho_1)^3}{2\pi\alpha N_c\chi''(\lambda_0)Y} \ . \tag{4.49}$$

We may also use (4.36) and (4.38) to evaluate the ρ-dependence of ρ_1 and ρ_2. It is straightforward to see that

$$\frac{d\rho_1(Y)}{d\rho} = \zeta + \mathcal{O}\left(\frac{1}{\rho_2-\rho_1}\frac{d(\rho_2-\rho_1)}{d\rho}\right) \tag{4.50}$$

and

$$\frac{d\rho_2(Y)}{d\rho} = 1 + \mathcal{O}\left(\frac{1}{\rho_2-\rho_1}\frac{d(\rho_2-\rho_1)}{d\rho}\right) \ . \tag{4.51}$$

Thus

$$\frac{d(\rho_2(Y)-\rho_1(Y))}{d\rho} \equiv \frac{d(\rho_2-\rho_1)}{d\rho} = 1-\zeta + \mathcal{O}\left(\frac{1}{\rho_2-\rho_1}\frac{d(\rho_2-\rho_1)}{d\rho}\right) \ . \tag{4.52}$$

Dropping the small term of the right hand side of (4.52) and using (4.49), one finds

$$\frac{d(\rho_2-\rho_1)}{d\rho} = \frac{(1-\lambda_0)(\rho_2-\rho_1)^3}{2\pi\alpha N_c\chi''(\lambda_0)Y}\left[1+\frac{(1-\lambda_0)(\rho_2-\rho_1)^3}{2\pi\alpha N_c\chi''(\lambda_0)Y}\right]^{-1} \ . \tag{4.53}$$

While an exact solution of (4.53) looks difficult, it is easy to see the general features of the solution.

When ρ is not too large the solution to (4.53), neglecting the final factor $[\ ]^{-1}$, is

$$\rho_2-\rho_1 = \frac{\Delta\rho}{\sqrt{1-\frac{(1-\lambda_0)(\rho_2-\rho_1)^2}{\pi\alpha N_c\chi''(\lambda_0)Y}\left(\rho-\hat{\rho}_1(Y)-\frac{1}{1-\hat{\lambda}_d}\right)}} \ . \tag{4.54}$$

Eq. (4.54) is valid until $\rho_2-\rho_1$ becomes on the order of $(\alpha Y)^{1/3}$ at which point the character of the ρ-dependence changes and $\zeta \to 0$ giving

$$\rho_1(Y) \approx \text{const}' \tag{4.55}$$

$$\rho_2(Y) \approx \rho + \text{const}'' \ . \tag{4.56}$$

Also, since

$$\frac{d(\rho-\rho_d(Y))}{d\rho} = 1-\zeta \approx \frac{d(\rho_2-\rho_1)}{d\rho} \tag{4.57}$$

one has

$$\rho-\rho_d(Y) = \rho_2-\rho_1+\text{const} \tag{4.58}$$

so that T, as given by (4.29), stays very close to the value $2\pi x^2 c$ starting at $\rho = \hat{\rho}_1(Y)+\frac{1}{1-\hat{\lambda}_d}$ up to $\rho = \hat{\rho}_1(Y)+\frac{1}{1-\hat{\lambda}_d}+\mathcal{O}\left(\frac{\pi\alpha N_c\chi''(\lambda_0)Y}{(1-\lambda_0)(\Delta\rho)^3}\right)$. This means that the saturation momentum for the scattering of the dipole x' on the dipole x at rapidity Y is

$$\begin{aligned}\rho_s(Y) &= \hat{\rho}_1(Y)+\frac{1}{1-\hat{\lambda}_d}+c_s\frac{\pi\alpha N_c\chi''(\lambda_0)Y}{(1-\lambda_0)(\Delta\rho)^3}\\ &= \hat{\rho}_{is}(Y)+c_s\frac{\pi\alpha N_c\chi''(\lambda_0)Y}{(1-\lambda_0)(\Delta\rho)^3}\end{aligned} \tag{4.59}$$

with c_s a matter of choice. While (4.59) indicates, parametrically, a small percentage deviation from the ρ_s that occurs using the Kovchegov equation that deviation is very significant. The c_s in (4.59) is determined by the exact value of T at which one declares saturation to have occured. Varying the value of T by, say, 2 will vary c_s by a similar factor which also means that T is a function of $[\rho-\rho_s(Y)]/(\alpha Y/(\Delta\rho)^3)$ and does not have the usual scaling behavior of the Kovchegov equation.

Finally, it is a little curious, and perhaps unexpected, that one now has a very extended region in ρ where T is near its unitarity limit and where our formalism applies. This is not the case with the Kovchegov equation. As ρ varies from $\hat{\rho}_1(Y)$ to $\rho_s(Y)$ the interval $\rho_2-\rho_1$ hardly changes and so the description of T hardly changes. What is happening is that the evolution from $y=0$ to $y=Y$, for a given ρ, has a fairly well defined scale of gluons at each intermediate value of y which contribute to the evolution. When ρ changes the scale of the intermediate gluons also changes, but the form of the dynamics remains exactly the same. In this picture unitarity limits involve a rather well defined scale of gluons at each value of y, but that scale depends on the initial and final dipole sizes.

4.3 Consistency checks

In this section we show that out result for the scattering amplitude (4.29) is boost-invariant. If the saturation boundaries which are fixed by x, x' and Y are used for any evolution step in rapidity between 0 and Y (global saturation boundaries as in sec. 3.3.2), then the amplitude (4.29) obeys also the completeness relation.

Let us start with the completeness relation (3.20). The dipole number density on the left-hand side of (3.20) can be calculated analogous to the scattering amplitude in the previous section and in the case where $x > x'$ it is

$$\begin{aligned} n(x,x',Y) &= \frac{4}{\rho_2-\rho_1}\left(\frac{x^2}{x'^2}\right)\left[Q_d^2(Y)\,x'^2\right]^{1-\lambda_d} \\ &\quad\times\sin\left(\frac{\pi(\tilde\rho(0)-\rho_1(0))}{\rho_2-\rho_1}\right)\sin\left(\frac{\pi(\ln(x^2/x'^2)-\rho_1(Y))}{\rho_2-\rho_1}\right)\ . \end{aligned} \tag{4.60}$$

Using this expression, the right-hand side of (3.20) becomes

$$\begin{aligned} &[\text{rhs of (3.20)}] = \frac{16}{(\rho_2-\rho_1)^2}\int\frac{d^2r_2}{2\pi r_2^2} \\ &\times\left(\frac{x^2}{r_2^2}\right)\left[Q_d^2(Y/2)\,r_2^2\right]^{1-\lambda_d}\sin\left(\frac{\pi(\tilde\rho(0)-\rho_1(0))}{\rho_2-\rho_1}\right)\sin\left(\frac{\pi(\ln(x^2/r_2^2)-\rho_1(Y/2))}{\rho_2-\rho_1}\right) \\ &\times\left(\frac{r_2^2}{x'^2}\right)\left[\hat Q_d^2(Y/2)\,x'^2\right]^{1-\lambda_d}\sin\left(\frac{\pi(\ln(x^2/r_2^2)-\rho_1(Y/2))}{\rho_2-\rho_1}\right)\sin\left(\frac{\pi(\ln(x^2/x'^2)-\rho_1(Y))}{\rho_2-\rho_1}\right), \end{aligned} \tag{4.61}$$

where $Q_d^2(Y/2)$ is given by (4.19), with Y replaced by $Y/2$, and $\hat Q_d^2(Y/2)$ is determined by matching the the two evolution steps at $Y/2$,

$$\hat Q_d^2(Y/2)\,r_2^2 = Q_d^2(Y/2)\,x^2\ . \tag{4.62}$$

This equation and $\xi = \ln(x^2/r_2^2)$ allow us to write the amplitude (4.61) as

$$\begin{aligned} [\text{rhs of (3.20)}] &= \frac{16}{(\rho_2-\rho_1)^2}\left(\frac{x^2}{x'^2}\right)\left[Q_d^2(Y)\,x'^2\right]^{1-\lambda_d} \\ &\quad\times\sin\left(\frac{\pi(\tilde\rho(0)-\rho_1(0))}{\rho_2-\rho_1}\right)\sin\left(\frac{\pi(\ln(x^2/x'^2)-\rho_1(Y))}{\rho_2-\rho_1}\right) \\ &\quad\times\int_{\rho_1(Y/2)}^{\rho_2(Y/2)}\frac{d\xi}{2}\sin^2\left(\frac{\pi(\xi-\rho_1(Y/2))}{\rho_2-\rho_1}\right) \end{aligned}$$

which after the integration over ξ,

$$\int_{\rho_1(Y/2)}^{\rho_2(Y/2)}\frac{d\xi}{2}\sin^2\left(\frac{\pi(\xi-\rho_1(Y/2))}{\rho_2-\rho_1}\right) = \frac{\rho_2-\rho_1}{4}, \tag{4.63}$$

agrees with (4.60). Thus, our formalism satisfies the completeness relation.

Now let us calculate the scattering amplitude of two dipoles in the c.m. frame starting with (3.16). To do this, in addition to $n(x,r_2,Y/2)$ given by (4.60), we need

also the dipole number density $n(x', r_2, Y/2)$ with $x' < r_2$. The later is obtained in the same way as the scattering amplitude (4.31) in the previous section and it is

$$\begin{aligned} n(x', r_2, Y/2) &= \frac{4}{\rho_2 - \rho_1} \left[\frac{1}{\tilde{Q}_d^2(Y/2)\, r_2^2} \right]^{1-\lambda_d} \\ &\times \sin\left(\frac{\pi(\rho_2(Y) - \ln(x^2/x'^2))}{\rho_2 - \rho_1} \right) \sin\left(\frac{\pi(\rho_2(Y/2) - \ln(x^2/r_2^2))}{\rho_2 - \rho_1} \right) \end{aligned} \tag{4.64}$$

where $\tilde{Q}_d^2(Y)$ is determined by

$$Q_d^2(Y)\, x'^2 = \frac{1}{\tilde{Q}_d^2(Y)\, x^2} \tag{4.65}$$

with $Q_d^2(Y)$ given in (4.19). Inserting the dipole number densities in (2.9), the scattering amplitude in c.m. frame becomes

$$\begin{aligned} T(x, x', Y) &= \frac{\pi\alpha^2}{2\lambda_d^2(1-\lambda_d)^2} \frac{16}{(\rho_2 - \rho_1)^2} \int \frac{d^2 r_2}{2\pi} \\ &\times \left(\frac{x^2}{r_2^2} \right) \left[Q_d^2(Y/2)\, r_2^2 \right]^{1-\lambda_d} \sin\left(\frac{\pi(\tilde{\rho}(0) - \rho_1(0))}{\rho_2 - \rho_1} \right) \sin\left(\frac{\pi(\ln(x^2/r_2^2) - \rho_1(Y/2))}{\rho_2 - \rho_1} \right) \\ &\times \left[\frac{1}{\tilde{Q}_d^2(Y/2)\, r_2^2} \right]^{1-\lambda_d} \sin\left(\frac{\pi(\rho_2(Y) - \ln(x^2/x'^2))}{\rho_2 - \rho_1} \right) \sin\left(\frac{\pi(\rho_2(Y/2) - \ln(x^2/r_2^2))}{\rho_2 - \rho_1} \right) . \end{aligned} \tag{4.66}$$

With (4.65), the variable $\xi = \ln(x^2/r_2^2)$ and the equality

$$\begin{aligned} \sin\left(\frac{\pi(\rho_2(Y) - \ln(x^2/x'^2))}{\rho_2 - \rho_1} \right) \sin\left(\frac{\pi(\rho_2(Y/2) - \ln(x^2/r_2^2))}{\rho_2 - \rho_1} \right) = \\ \sin\left(\frac{\pi(\ln(x^2/x'^2) - \rho_1(Y))}{\rho_2 - \rho_1} \right) \sin\left(\frac{\pi(\ln(x^2/r_2^2) - \rho_1(Y/2))}{\rho_2 - \rho_1} \right) , \end{aligned} \tag{4.67}$$

the amplitude (4.66) reads

$$\begin{aligned} T(x, x', Y) &= \frac{\pi\alpha^2 x^2}{2\lambda_d^2(1-\lambda_d)^2} \frac{16}{(\rho_2 - \rho_1)^2} \left[Q_d^2(Y)\, x'^2 \right]^{1-\lambda_d} \\ &\times \sin\left(\frac{\pi(\tilde{\rho}(0) - \rho_1(0))}{\rho_2 - \rho_1} \right) \sin\left(\frac{\pi(\ln(x^2/x'^2) - \rho_1(Y))}{\rho_2 - \rho_1} \right) \\ &\times \int_{\rho_1(Y/2)}^{\rho_2(Y/2)} \frac{d\xi}{2} \sin^2\left(\frac{\pi(\xi - \rho_1(Y/2))}{\rho_2 - \rho_1} \right) . \end{aligned} \tag{4.68}$$

After the integration over ξ (see eq. (4.63)), the resulting scattering amplitude agrees with the result for the scattering amplitude obtained in the laboratory frame (4.29).

5 BFKL evolution with running coupling and boundaries

We now add a running coupling to the discussion of Sec. 4. It is difficult to use a global version of BFKL evolution, covering all Y-values, such as given in (4.22), so we shall instead use a more local approach. The boundaries ρ_1 and ρ_2 of Fig. 8 are now no longer straight lines, however, the problem can still be formulated in terms of a similar picture with curved boundaries to be determined. BFKL evolution goes from x at $y = 0$ to x' at $y = Y$. Between ρ_1 and ρ_2 the normal BFKL kernel is used, but we demand a solution which vanishes on the boundaries. The scattering amplitude thus depends on x, x' and Y, the variables fixing the region of evolution. In order to do the actual calculation additional variables z and y are introduced. z and y are the dipole size and rapidity of an intermediate stage in the evolution between x and x'. The BFKL evolution is written in terms of z and y. In fixed coupling evolution these intermediate stages of evolution were not so visible because we were able to identify the part of the BFKL equation that corresponded to diffusion, and then it was possible to combine the results of global BFKL evolution, as given in (4.25), with the solution to the diffusion equation with boundaries, given in (4.15). We note, however, that T as given in (4.29) does not obey BFKL evolution, say in the variables x' and Y, because a variation of these variables changes the boundaries. The solution (4.29) represents evolution between x at $y = 0$ and x' at $y = Y$ for fixed x, x' and Y and it is this problem that we now turn to in case the coupling runs.

With the variables x, x' and Y being fixed we consider the scattering amplitude $T(z, y)$ going from x at $y = 0$ to z at y, obeying the BFKL equation, and vanishing on the boundaries $\rho_1(y)$, $\rho_2(y)$. Because running of the coupling introduces an explicit scale it is convenient to now use variables scaled by Λ^2 rather than by x^2. Thus in this section our notation is

$$\begin{aligned} \rho_i &= \ln\left(1/\Lambda^2 x^2\right), \quad \rho_f = \ln\left(1/\Lambda^2 x'^2\right), \quad \rho = \ln\left(1/\Lambda^2 z^2\right) \\ \rho_d &= \ln\left(Q_d^2/\Lambda^2\right), \quad \rho_1 = \ln\left(Q_1^2/\Lambda^2\right), \quad \rho_2 = \ln\left(Q_2^2/\Lambda^2\right) \end{aligned} \tag{5.1}$$

where Q_1 and Q_2 are the momenta setting the boundaries, and ρ_i and ρ_f represent the initial and final dipole sizes.

The BFKL equation takes the form

$$\frac{\partial}{\partial y}\left[T/\alpha\right] = \frac{\alpha N_c}{\pi} K \times \left[T/\alpha\right] \tag{5.2}$$

with K the usual BFKL kernel. The convolution indicated in (5.2) can be written

more fully as

$$[K \times f](\rho) = \int_{-\infty}^{\infty} d\rho' K(\rho, \rho') f(\rho') \ . \tag{5.3}$$

The BFKL kernel is given as

$$K(\rho, \rho') = \int \frac{d\lambda}{2\pi i} \, e^{-(1-\lambda)(\rho-\rho')} \, 2\chi(\lambda) \tag{5.4}$$

and we look for a solution to (5.2) where $T(\rho, y)$ vanishes when $\rho = \rho_1, \rho_2$. The running coupling is given, as usual, by

$$\alpha(\rho) = \frac{1}{b\rho} \ . \tag{5.5}$$

The problem of finding a solution to (5.2) with K given in (5.4) and where the solution vanishes at ρ_1 and ρ_2 is a well defined mathematical problem, but it appears too difficult to solve exactly. However, following Refs. [16] and [30] we can get an approximate solution to the problem by expanding $\chi(\lambda)$ in (5.4) about λ_d

$$\chi(\lambda) \approx \chi(\lambda_d) + (\lambda - \lambda_d) \, \chi'(\lambda_d) + \frac{1}{2}(\lambda - \lambda_d)^2 \, \chi''(\lambda_d) \tag{5.6}$$

in which case

$$K(\rho, \rho') \approx e^{-(1-\lambda_d)\rho} \, 2 \left[\chi(\lambda_d) + \chi'(\lambda_d) \frac{\partial}{\partial \rho} + \frac{1}{2} \chi''(\lambda_d) \, \frac{\partial^2}{\partial \rho^2} \right] e^{(1-\lambda_d)\,\rho} \delta(\rho - \rho') \tag{5.7}$$

with λ_d to be determined much as was done in Sec. 4.2.

Using (5.7) in (5.2) gives

$$\frac{\partial}{\partial y} \, [T/\alpha](\rho, y) = \frac{2N_c}{\pi b \rho} \, e^{-(1-\lambda_d)\rho} \left[\chi(\lambda_d) + \chi'(\lambda_d) \frac{\partial}{\partial \rho} + \frac{1}{2} \chi''(\lambda_d) \, \frac{\partial^2}{\partial \rho^2} \right] e^{(1-\lambda_d)\,\rho} \, [T/\alpha](\rho, y). \tag{5.8}$$

There are three distinct regions of parameters determining how, and to what extent, (5.8) can be solved:

$$\text{(i)} \quad \frac{\rho_2 - \rho_1}{Y^{1/6}} \gg 1 \tag{5.9}$$

$$\text{(ii)} \quad \frac{\rho_2 - \rho_1}{Y^{1/6}} \ll 1 \tag{5.10}$$

$$\text{(iii)} \quad \frac{\rho_2 - \rho_1}{Y^{1/6}} \approx 1 \ . \tag{5.11}$$

In region (i) expand the $1/\rho$ coming from the running coupling in (5.8) as

$$\frac{1}{\rho} = \frac{1}{\rho_d} - \frac{(\rho - \rho_d)}{\rho_d^2} \tag{5.12}$$

where, as in Sec. 4.2, $\rho_d(y) = \rho$ defines a line of constant T. Then (5.12) leads to diffusion in a linear potential. Condition (i) corresponds to an exponentially small amplitude near the boundary ρ_2 and the problem reduces to the problem of solving (5.8) with a single boundary at ρ_1 which has the solution given in Ref. [16]. In region (ii) one may replace $1/\rho$ by $1/\rho_d$ since the range $\rho_1 < \rho < \rho_2$ is so small that the linear potential has very little effect. In this region we can effectively use a fixed coupling equation locally in y, but one must take into account that ρ_d depends on y. We shall shortly carry this out in detail. It appears difficult to get an analytic solution in region (iii), but the form of the solution is strongly constraint by the known solution in region (i) and (ii).

Now we turn to the solution of (5.8) in region (ii) where ρ can be replaced by ρ_d. Since we expect the ρ-dependence of the solution to be the same, in form, to the fixed coupling case it is natural to write

$$T/\alpha = \sin\left(\frac{\pi(\rho-\rho_1)}{\rho_2-\rho_1}\right) f(\rho, y)\ . \tag{5.13}$$

In addition we suppose $\rho_2 - \rho_1$ is very weakly dependent on y so that (5.8) gives, with $\dot\rho_1 = d\rho_1/dy$,

$$-\frac{\pi\dot\rho_1}{\rho_2-\rho_1}\cos\left(\frac{\pi(\rho-\rho_1)}{\rho_2-\rho_1}\right) f + \sin\left(\frac{\pi(\rho-\rho_1)}{\rho_2-\rho_1}\right)\frac{\partial f}{\partial y} = \tag{5.14}$$
$$\frac{2N_c}{\pi b\rho_d}\, e^{-(1-\lambda_d)(\rho-\rho_d)}\left[\chi(\lambda_d) + \chi'(\lambda_d)\frac{\partial}{\partial\rho} + \frac{1}{2}\chi''(\lambda_d)\,\frac{\partial^2}{\partial\rho^2}\right] e^{(1-\lambda_d)(\rho-\rho_d)} \sin\left(\frac{\pi(\rho-\rho_1)}{\rho_2-\rho_1}\right) f.$$

Eq. (4.29) suggests that the ρ-dependence of f should be $e^{-(1-\lambda_d)(\rho-\rho_d)+\gamma\ln y}$, with the $\gamma\ln y$ term due to the fact that (5.14) is an equation for T/α not for T, in which case (5.14) gives

$$-\dot\rho_1 = \frac{2N_c}{\pi b\rho_d}\chi'(\lambda_d) \tag{5.15}$$

from the $\cos\left(\frac{\pi(\rho-\rho_1)}{\rho_2-\rho_1}\right)$ part of the equation, and

$$\frac{\gamma}{y} + (1-\lambda_d)\dot\rho_d = \frac{2N_c}{\pi b\rho_d}\left[\chi(\lambda_d) - \frac{1}{2}\chi''(\lambda_d)\frac{\pi^2}{(\rho_2-\rho_1)^2}\right] \tag{5.16}$$

coming from the $\sin\left(\frac{\pi(\rho-\rho_1)}{\rho_2-\rho_1}\right)$ part of the equation. The γ/y term in (5.16) is small and can be dropped. Since ρ_d defines a line of constant amplitude $\dot\rho_d$ and $\dot\rho_1$ must be exactly equal in which case (5.15) and (5.16) becomes identical to (4.16) and (4.17) when the form of the running coupling, (5.5), is taken into account.

Eqs. (5.15) and (5.16) give (4.18) along with

$$\frac{d}{dy}\rho_d^2 = \frac{4N_c}{\pi b}\frac{\chi(\lambda_d)}{1-\lambda_d}\left[1 - \frac{1}{2}\frac{\pi^2}{(\rho_2-\rho_1)^2}\frac{\chi''(\lambda_d)}{\chi(\lambda_d)}\right] \tag{5.17}$$

or

$$\rho_d(y) = \sqrt{\frac{4N_c}{\pi b}\frac{\chi(\lambda_d)}{1-\lambda_d}\left[1 - \frac{1}{2}\frac{\pi^2}{(\rho_2-\rho_1)^2}\frac{\chi''(\lambda_d)}{\chi(\lambda_d)}\right] y} + c_d \ . \tag{5.18}$$

The constant c_d in (5.18) follows not from solving (5.17), but reflects the fact that we have not systematically kept terms in (5.14) and in (5.17) of size $1/y$ and $1/\sqrt{y}$, respectively. One such term is the γ/y term in (5.16). Taking $\alpha(\rho) \approx [b(\rho_d + c')]^{-1}$ rather than $\alpha(\rho) \approx [b\rho_d]^{-1}$ would also give a contribution to c_d. In contrast to Ref. [16], here we do not have control over such terms. As before (4.18) gives λ_d, approximately as in (4.20), when $\rho_2 - \rho_1$ is large. Since ρ_d has the same y-dependence as ρ_1 and ρ_2 we can write

$$\rho_{1,2} = \sqrt{\frac{4N_c}{\pi b}\frac{\chi(\lambda_d)}{1-\lambda_d}\left[1 - \frac{1}{2}\frac{\pi^2}{(\rho_2-\rho_1)^2}\frac{\chi''(\lambda_d)}{\chi(\lambda_d)}\right] y} + c_{1,2} \ . \tag{5.19}$$

where c_d and c_1, c_2 can depend on ρ_i and ρ_f. From (5.13) and taking $\gamma = 1/2$ to guarantee the lack of y-dependence of T when $\rho - \rho_d$ is fixed, one can write

$$T(\rho, y) = 2\pi x^2 c \frac{(\rho_2-\rho_1)}{\pi} e(1-\lambda_d) \sin\left(\frac{\pi(\rho-\rho_1)}{\rho_2-\rho_1}\right) e^{-(1-\lambda_d)(\rho-\rho_1(y))} \ . \tag{5.20}$$

T, as given in (5.20) and with ρ_1 given in (5.19), satisfies the BFKL equation (5.2) as well as the boundary conditions. In addition

$$T(\rho_1(y) + \frac{1}{1-\lambda_d}, y) = 2\pi x^2 c \ . \tag{5.21}$$

Eq. (5.21) is a saturation, or unitarity, condition for evolution at intermediate values of the rapidity.

Eq. (5.20) is not so strong as our fixed coupling equation (4.29) which gives the amplitude for evolution from a given dipole of size x in terms of boundary lines ρ_1 and ρ_2 which then are completely determined in terms of the evolution. In the present case we are able to do the evolution at large rapidities, but we are unable to connect to the initial dipole, or hadron. Nevertheless, there is only one extra unknown constant here as compared to the fixed coupling case as we now demonstrate. First, we note that the relationship between $\rho_2(Y)$ and ρ_f is here essentially as it was in the fixed coupling case. In the fixed coupling case $\rho_2 - \rho_f$ was determined by symmetry from the determination of $\rho_1 - \rho_i$ which followed from

unitarity. However, we equally well could have determined ρ_2 by unitarity in which case the condition is

$$T(\rho = \rho_2(y) - \frac{1}{1-\lambda_d}, \rho_f, y) = 2\pi r_2^2 c \ . \tag{5.22}$$

where

$$r_2^2 = \frac{1}{\Lambda^2} e^{-(\rho_2(y) - \frac{1}{1-\lambda_d})} \ . \tag{5.23}$$

Eqs. (5.22) and (5.23) determine the curve $\rho_2(y)$ as the right-most value of ρ from which BFKL evolution respects the unitarity limit in going from ρ to ρ_f. Thus at the maximum rapidity (4.38), except for some notational changes required in the running coupling case, remains valid. That is

$$\rho_2(Y) = \rho_f + \frac{1}{1-\lambda_d} \ln \left[\frac{c\lambda_d^2 (1-\lambda_d)^3 (\rho_2 - \rho_1)^3 e}{\pi^2 \alpha^2 (\rho_2(Y) - \rho_f)} \right] \ . \tag{5.24}$$

Eq. (5.24) determines the constant c_2 in (5.19) to be

$$c_2 = \rho_f - \sqrt{\frac{4N_c}{\pi b} \frac{\chi(\lambda_d)}{1-\lambda_d} \left[1 - \frac{1}{2} \frac{\pi^2}{(\rho_2 - \rho_1)^2} \frac{\chi''(\lambda_d)}{\chi(\lambda_d)} \right] Y} + \frac{1}{1-\lambda_d} \ln \left[\frac{c\lambda_d^2 (1-\lambda_d)^3 (\rho_2 - \rho_1)^3 e}{\pi^2 \alpha^2 (\rho_2(Y) - \rho_f)} \right]. \tag{5.25}$$

However, we are not able to determine c_1. Determining c_1 requires evolving into regions where (5.10) is no longer valid and hence would require an ability to solve the BFKL equation keeping the running of the coupling as given in (5.13). We do not know how to do this.

One can get some insight into the regions demarcated by (5.9)-(5.11) by looking at $\rho_d(y)$ as given by (5.18) as one reduces y to the point where $\frac{\rho_2 - \rho_1}{y^{1/6}}$ is no longer so small. We can write

$$\rho_d(y) \approx \sqrt{\frac{4N_c}{\pi b} \frac{\chi(\lambda_d)}{1-\lambda_d} y} \left[1 - \frac{1}{4} \frac{\pi^2}{(\rho_2 - \rho_1)^2} \frac{\chi''(\lambda_d)}{\chi(\lambda_d)} \right] \ . \tag{5.26}$$

When $\frac{\rho_2 - \rho_1}{y^{1/6}}$ is of order 1, ρ_d has a dominant $\sqrt{y}$ term along with a term of size $y^{1/6}$. But, this is exactly what happens in the region (5.9) as seen in the solution of Ref. [16]. Thus when $\frac{\rho_2 - \rho_1}{y^{1/6}}$ is of order 1 there are $y^{1/6}$ corrections coming both from the boundaries and from the linear potential. When $\frac{\rho_2 - \rho_1}{y^{1/6}} \gg 1$ the linear potential effects dominate the effects due to the ρ_2 boundary. When $\frac{\rho_2 - \rho_1}{y^{1/6}} \ll 1$ the boundary effects dominate the linear potential effects.

Acknowledgements

A. Sh. acknowledges financial support by the Deutsche Forschungsgemeinschaft under contract Sh 92/1-1.

References

[1] L. V. Gribov, E. M. Levin and M. G. Ryskin, Phys. Rept. **100** (1983) 1.

[2] Y. V. Kovchegov, A. H. Mueller and S. Wallon, Nucl. Phys. B **507** (1997) 367.

[3] E. A. Kuraev, L. N. Lipatov and V. S. Fadin, Sov. Phys. JETP **45** (1977) 199.

[4] I. I. Balitsky and L. N. Lipatov, Sov. J. Nucl. Phys. **28** (1978) 822.

[5] Y. L. Dokshitzer, Sov. Phys. JETP **46** (1977) 641.

[6] V. N. Gribov and L. N. Lipatov, Yad. Fiz. **15** (1972) 781 [Sov. J. Nucl. Phys. **15** (1972) 438].

[7] G. Altarelli and G. Parisi, Nucl. Phys. B **126** (1977) 298.

[8] For reviews see: E. Iancu, A. Leonidov and L. McLarren in "QCD Perspectives on Hot and Dense Matter", J.-P. Blaizot and E. Iancu eds., Kluwer Academic Publishers (2002), hep-ph/0202270; A. Mueller in "QCD Perspectives on Hot and Dense Matter", J.-P. Blaizot and E. Iancu eds., KluwerAcademic Publishers (2002), hep-ph/0111244; E. Iancu and R. Venugopalan, hep-ph/0303204.

[9] R. Baier, A. H. Mueller, D. Schiff and D. T. Son, Phys. Lett. B **502** (2001) 51; Phys. Lett. B **539** (2002) 46.

[10] I. Balitsky, Nucl. Phys. B **463** (1996) 99; Phys. Rev. Lett. **81** (1998) 2024; Phys. Lett. B **518** (2001) 235.

[11] J. Jalilian-Marian, A. Kovner, A. Leonidov and H. Weigert, Nucl. Phys. B **504** (1997) 415; Phys. Rev. D **59** (1999) 014014.

[12] E. Iancu, A. Leonidov and L. D. McLerran, Phys. Lett. B **510** (2001) 133; Nucl. Phys. A **692** (2001) 583.

[13] H. Weigert, Nucl. Phys. A **703** (2002) 823.

[14] K. Rummukainen and H. Weigert, "Universal features of JIMWLK and BK evolution at small x," arXiv:hep-ph/0309306.

[15] Y. V. Kovchegov, Phys. Rev. D **60** (1999) 034008; Phys. Rev. D **61** (2000) 074018.

[16] A. H. Mueller and D. N. Triantafyllopoulos, Nucl. Phys. B **640** (2002) 331.

[17] D. N. Triantafyllopoulos, Nucl. Phys. B **648** (2003) 293.

[18] A. H. Mueller, Nucl. Phys. B **558** (1999) 285.

[19] E. Iancu, K. Itakura and L. McLerran, Nucl. Phys. A **708** (2002) 327.

[20] K. Golec-Biernat, L. Motyka and A. M. Stasto, Phys. Rev. D **65** (2002) 074037.

[21] S. Munier and R. Peschanski, Phys. Rev. Lett. **91** (2003) 232001; "Traveling wave fronts and the transition to saturation," arXiv:hep-ph/0310357.

[22] E. Levin and K. Tuchin, Nucl. Phys. B **573** (2000) 833.

[23] E. Iancu and A. H. Mueller, Nucl. Phys. A **730** (2004) 494.

[24] G. P. Salam, Nucl. Phys. B **461** (1996) 512.

[25] A. H. Mueller, Nucl. Phys. A **724** (2003) 223.

[26] A. H. Mueller, "Small-x physics, high parton densities and parton saturation in QCD," arXiv:hep-ph/9911289.

[27] A. H. Mueller, Nucl. Phys. B **415** (1994) 373.

[28] S. Munier and A. Shoshi, "Diffractive photon dissociation in the saturation regime from the Good and Walker picture," arXiv:hep-ph/0312022.

[29] A. H. Mueller, "Parton saturation: An overview," arXiv:hep-ph/0111244.

[30] G. Camici and M. Ciafaloni, Phys. Lett. B **395** (1997) 118.